Electronic Supplementary Material (ESI) for Inorganic Chemistry Frontiers.

Supplementary Information

Unexpected and frustrating transformations of double-decker silsesquioxanes

Monika Rzonsowska, Katarzyna Mituła, Julia Duszczak, Małgorzata Kasperkowiak, Rafał Januszewski, Anita Grześkiewicz, Maciej Kubicki, Daria Głowacka and Beata Dudziec*

Table of Contents

1. Experimental Procedures

1.1 Measurements

Nuclear Magnetic Resonance (NMR)
^{1}H, ^{13}C, and ^{29}Si Nuclear Magnetic Resonance (NMR) were performed on Brucker Ultra Shield 400 and 300 spectrometers using $CDCl_3$ and CD_2Cl_2 as solvents. Chemical shifts are reported in ppm with reference to the residual solvents peaks for ^{1}H and ^{13}C and to TMS for ^{29}Si NMR.

FT-IR spectroscopy
Fourier Transform-Infrared (FT-IR) spectra were recorded on a Nicolet iS5 (Thermo Scientific) spectrophotometer equipped with a diamond ATR unit. In all cases, 16 scans at a resolution of 2 cm^{-1} were collected, to record the spectra in a range of 4000-450cm^{-1}.

ESI-TOF MS
High resolution mass spectra (HRMS) were obtained using Impact HD mass spectrometer (Q-TOF type instrument equipped with electrospray ion source; Bruker Daltonics, Germany). The sample solutions (DCM/MeOH) were infused into the ESI source by a syringe pump (direct inlet) at the flow rate of 3 µL/min. The instrument was operated under the following optimized settings: end plate voltage 500 V; capillary voltage 4.2 kV; nebulizer pressure 0.3 bar; dry gas (nitrogen) temperature 200°C; dry gas flow rate 4 L/min. The spectrometer was previously calibrated with the standard tune mixture.

MALDI-TOF MS
Matrix assisted laser desorption ionization time of flight (MALDI-TOF) mass spectrometry was performed using a Ultraflex TOF/TOF (Bruker Daltonics, Germany) in reflection mode. The thin-layer preparation method was applied. The matrix (2,5-dihydroxybenzoic acid - DHB) was dissolved at a concentration of 20 mg/mL in mixture of 0.1% TFA in de-ionized water (70 % v/v) and acetonitrile (30% v/v). The matrix solution was spotted onto the target and dried in air. In the next step sample solution (2 mg/mL in DCM) was deposited onto the matrix spot and dried in air.

Elemental analyses (EA)
Elemental analyses were performed using a Vario EL III instrument (Elementar Analysensysteme GmbH, Langenselbold, Germany).

Thermogravimetric Analysis (TGA)
TGA analyses were performed using a TGA4000 (Perkin Elmer) with thermal gravimetric analyzer. The measurements were conducted in nitrogen atmosphere (flow of 20 mL/min), from 30°C to 995°C, at the heating rate of 10°C/min. The temperature of initial degradation (Td) was taken as the onset temperature at which 5 wt% of mass loss occurs.

X-ray crystallography
Diffraction data were collected by the ω-scan technique, using for SQ-T1d mirror-monochromated CuKα radiation (λ=1.54178 Å), at 130(1) on Rigaku SuperNova four-circle diffractometer with Atlas CCD detector, and in all other cases with graphite-monochromated MoKα radiation (λ=0.71073 Å), at 100(1) (for SQ-Dm2d at room temperature) on Rigaku XCalibur four-circle diffractometer with EOS CCD detector. The data were corrected for Lorentz-polarization as well as for absorption effects.[1] Precise unit-cell parameters were determined by a least-squares fit of the reflections of the highest intensity, chosen from the whole experiment. The structures were solved with SHELXT [2] and refined with the full-matrix least-squares procedure on F_2 by SHELXL.[3] All non-hydrogen atoms were refined anisotropically. All hydrogen atoms were placed in idealized positions and refined as 'riding model' with isotropic displacement parameters set at 1.2 (1.5 for CH_3) times Ueq of appropriate carrier atoms. The crystals of SQ-T1a and SQ-T1d turned out to be twinned, and this was considered both during data reduction and structure refinement. BASF parameter, indicating the mutual content of two components, refined at 0.5048(5) in SQ-T1a and at 0.455(4) in SQ-T1d. In structures SQ-Td1a, SQ-Dm2b and SQ-T1b-SC, SQ-Td1c-SC and SQ-Td1c (especially heavy disorder) certain fragments of the structures have been disordered over two or even three positions, and alternatives were refined with a number of restraints. In SQ-Dm2a and SQ-T1b-SC the huge regions of diffused electron density were found; as the attempts of modelling the solvent molecules were unsuccessful, the SQUEEZE modelling of these diffused electron density was applied.[4] In some cases, restraints or constraints for the displacement ellipsoids were also applied.

Crystallographic data for the structural analysis has been deposited with the Cambridge Crystallographic Data Centre. Copies of this information may be obtained free of charge from: The Director, CCDC, 12 Union Road, Cambridge, CB2 1EZ, UK; e-mail: deposit@ccdc.cam.ac.uk, or www: www.ccdc.cam.ac.uk.

2. Additional spectra

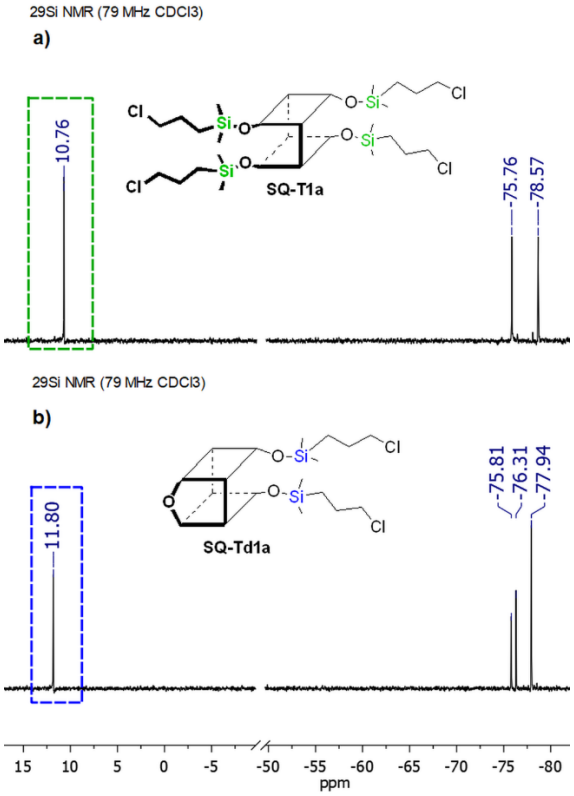

Figure S 1 ^{29}Si NMR spectra of a) SQ-T1a and b) SQ-Td1a.

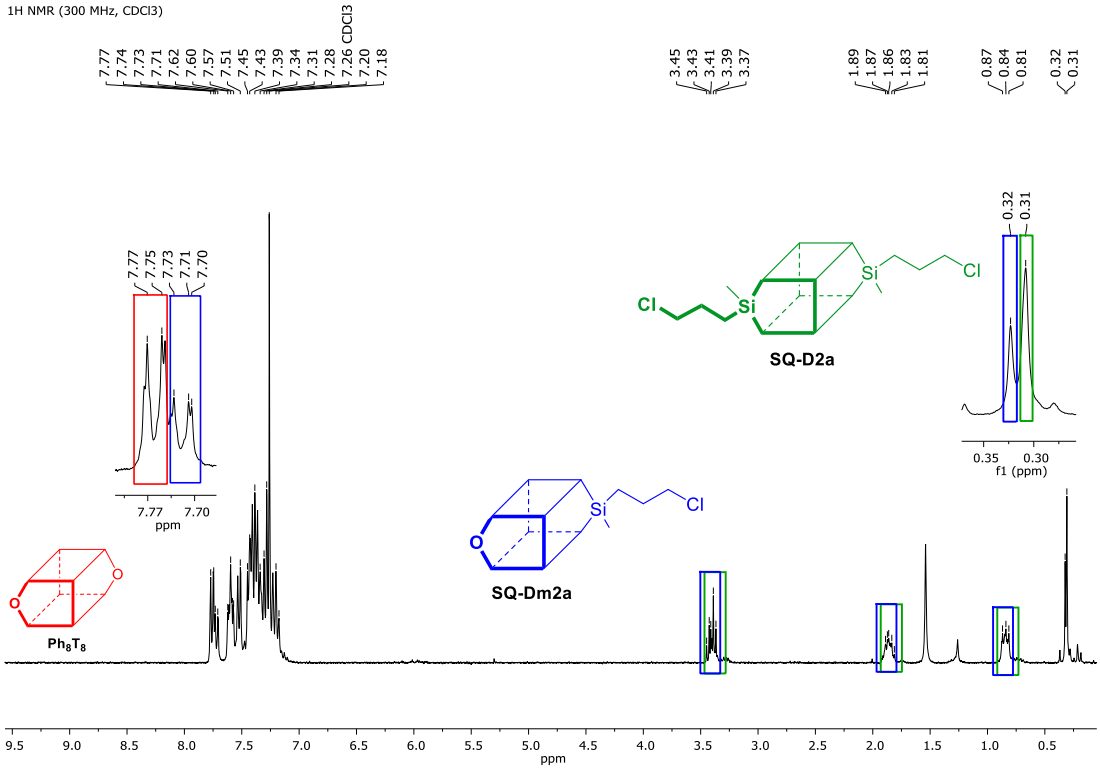

Figure S 2 ^{1}H NMR spectra of post-reaction mixture of hydrolytic condensation of SQ-4OH with 2a.

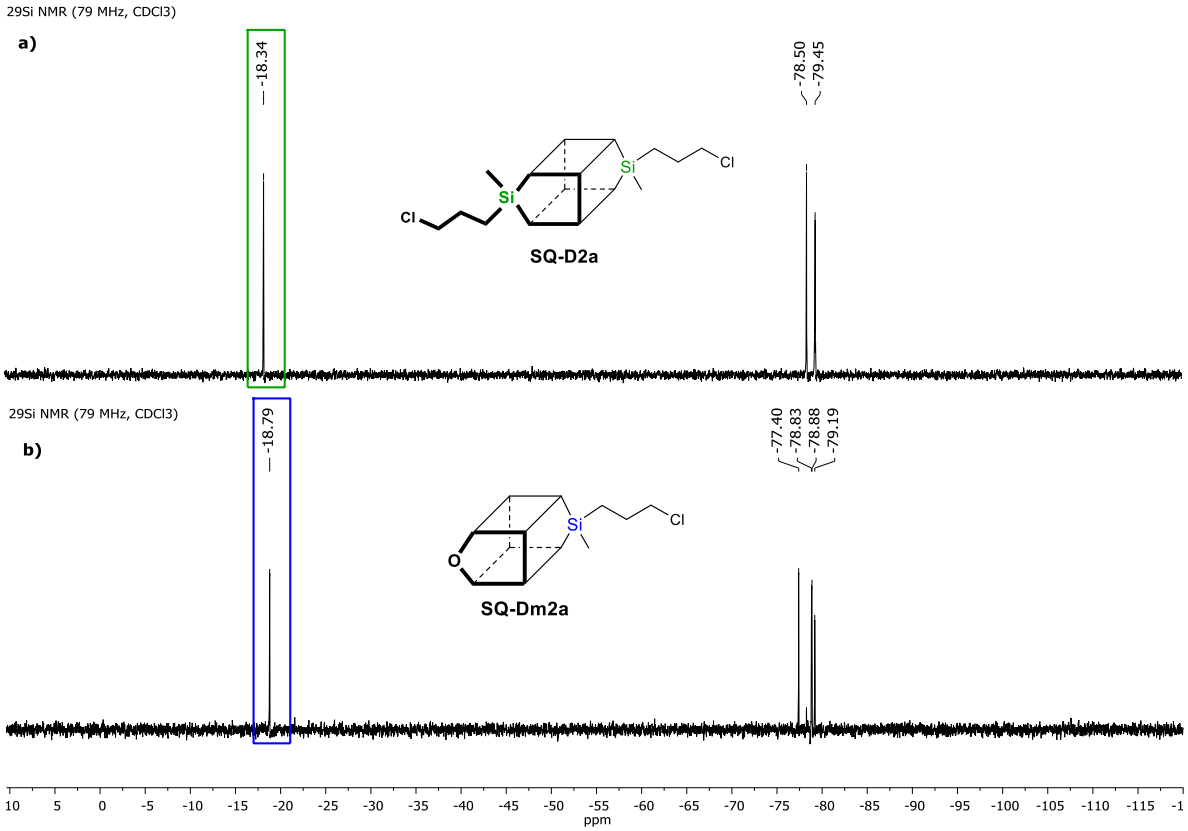

Figure S 3 ^{29}Si NMR spectra's of a) SQ-D2a and b) SQ-Dm2a.

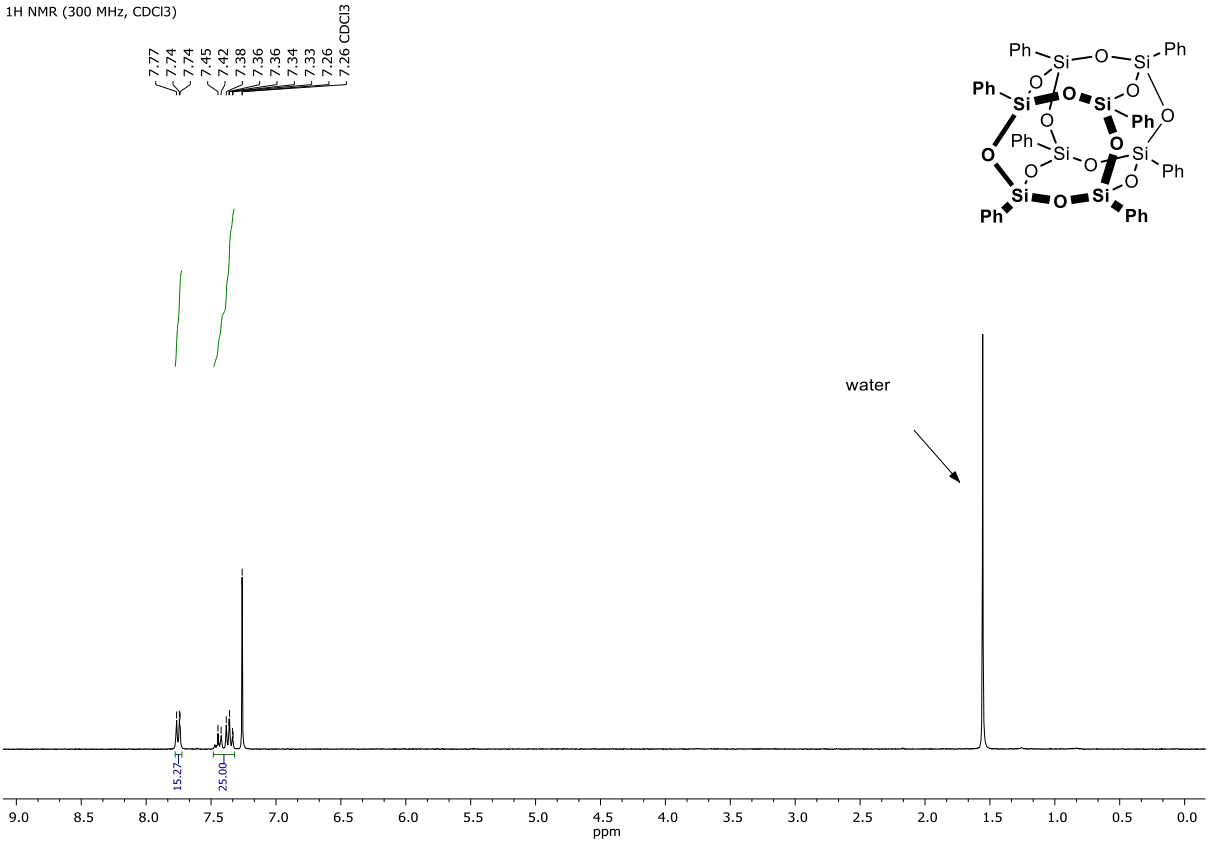

Figure S 4 ^{1}H NMR spectrum of Ph_8T_8 in $CDCl_3$, 300 MHz.

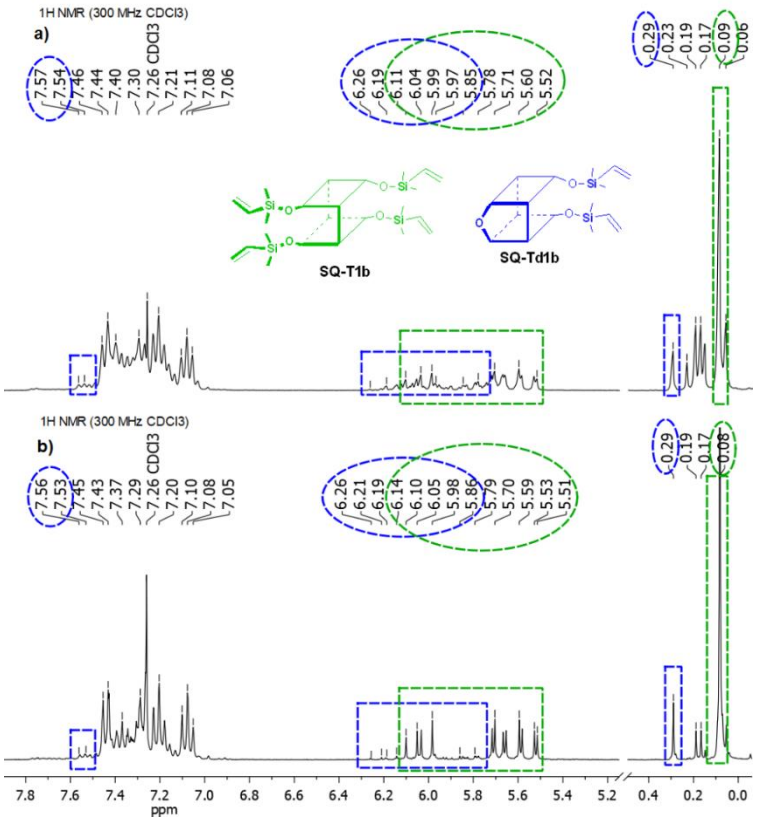

Figure S 1 Stacked ^{1}H NMR spectra of **SQ-T1b** hydrolytic condensation reaction mixtures measured after a) 4 h and b) 20 h.

3. The list of obtained products

Table S 1 The list of obtained products with their yields and respective chlorosilane used

Chlorosilane	Structures of obtained compounds [Yield (%)]	
1a	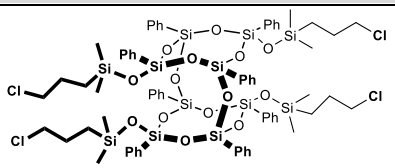 **SQ-T1a, pp. S8-S9** [68]	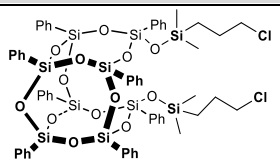 **SQ-Td1a, pp. S10-S11** [18]
1b	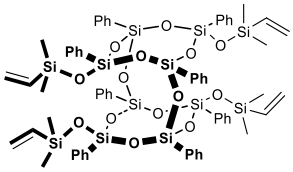 **SQ-T1b, pp. S12 [90]**	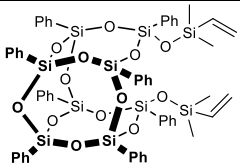 **SQ-Td1b, pp. S12-S13 [8]**
1c	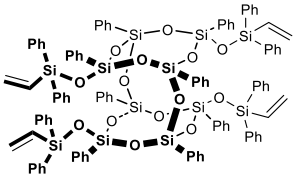 **SQ-T1c, pp. S14 [65]**	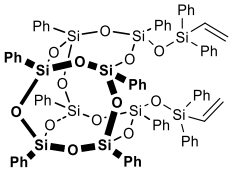 **SQ-Td1c, pp. S14-S15 [25]**
1d	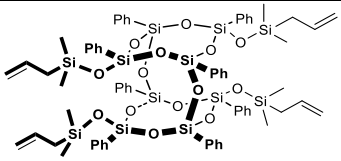 **SQ-T1d, pp. S16 [69]**	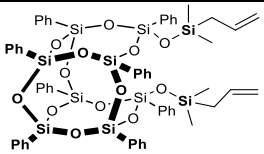 **SQ-Td1d, pp. S17-S18 [15]**
2a	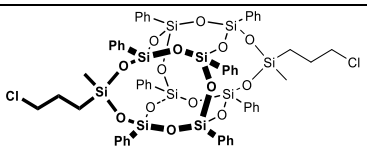 **SQ-D2a, pp. S19 [70]**	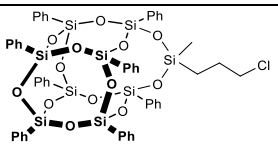 **SQ-Dm2a, pp. S19-S20 [15]**
2b	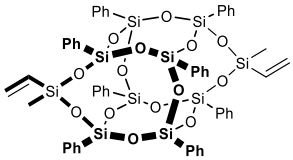 **SQ-D2b, pp. S21 [78]**	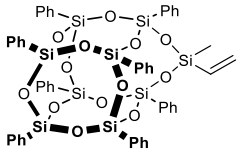 **SQ-Dm2b, pp. S21-S22 [6]**
2d	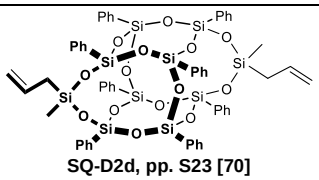 **SQ-D2d, pp. S23 [70]**	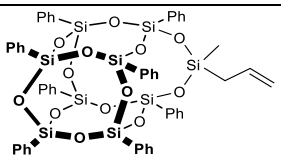 **SQ-Dm2d, pp. S23-S24 [12]**
	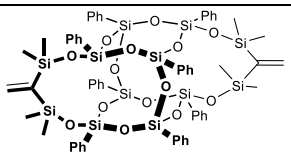 **SQ-T1b-SC, pp. S29-S31 [89]**	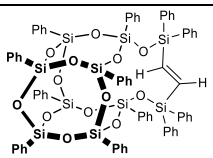 **SQ-Td1c-SC, pp. S32-S34 [85]**

4. Data characterizing the obtained products and copies of ^{1}H, ^{13}C, ^{29}Si NMR spectra

SQ-T1a

White solid. Isolated Yield 68%.

^{1}H NMR ($CDCl_3$, 300 MHz): δ/ppm = 7.45-7.13 (m, 40H, Ph), 3.00 (t, *J* = 6.9 Hz, 8H), 1.52-1.44 (m, 8H, $-CH_2-$), 0.56-0.50 (m, 8H, $-SiCH_2-$), 0.02 (s, 24H, $-Si(CH_3)_2$).
^{13}C NMR ($CDCl_3$, 101 MHz): δ/ppm = 134.38, 134.31, 133.16, 131.45, 130.56, 130.20, 127.91, 127.75 (Ph), 47.73 ($-CH_2-Cl$), 26.84 ($-CH_2-$), 15.88 ($-SiCH_2-$), 0.19 ($-Si(CH_3)_2$).
^{29}Si NMR ($CDCl_3$, 79 MHz): δ/ppm = 10.76 ($-Si(CH_3)_2$), -75.76, -78.57.
IR (ATR, cm-1): 3072.26, 3050.65 (C-H phenyl), 3005.38 (=C-H), 2953.48 (C-H), 1593.35, 1429.50 (C=C phenyl), 1251.85 (Si-C), 1126.64, 1096.14, 1040.23 (Si-O-Si), 997.63 (C-H phenyl).
EA: Anal. calcd for $C_{68}H_{88}Cl_4O_{14}Si_{12}$ (%):C, 50.78, H, 5.52; found: C, 50.89; H, 5.63.
ESI-MS: Calcd. for $C_{68}H_{88}Cl_4Na^{+}O_{14}Si_{12}$: *m/z* 1627.2052 [M + Na^{+}]. Found: 1627.2077.

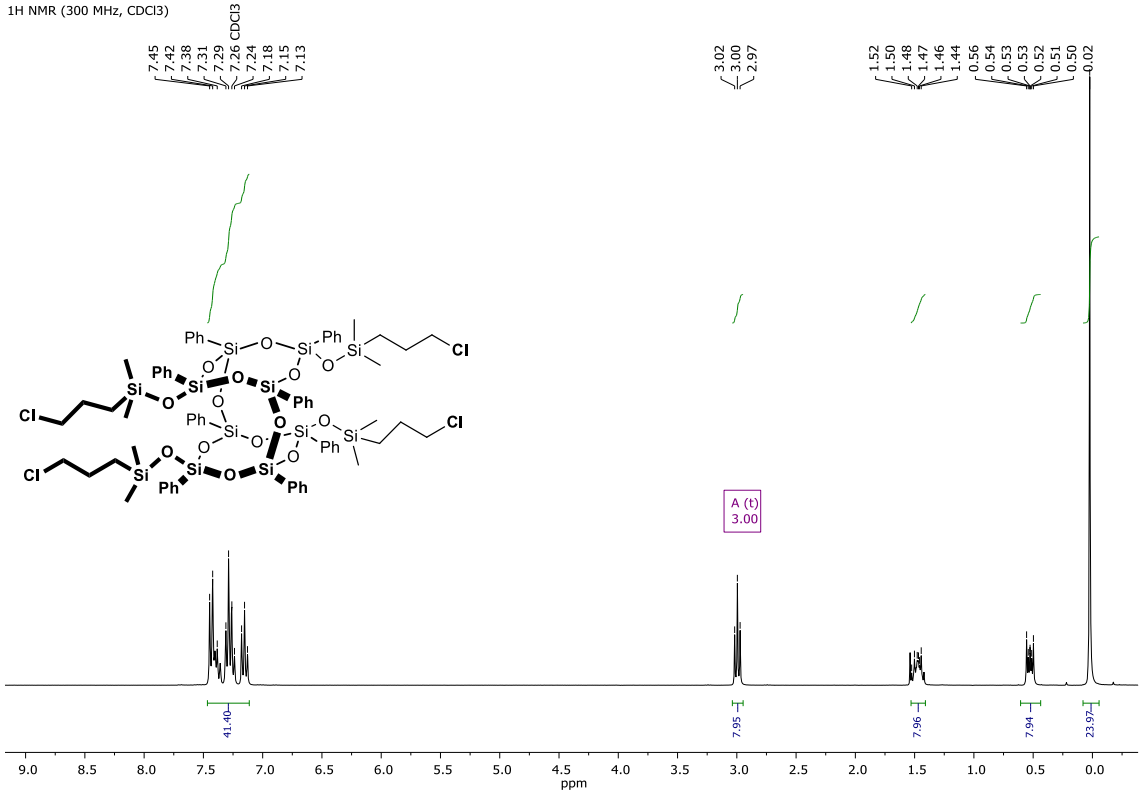

Figure S 2 ^{1}H NMR spectrum of SQ-T1a in $CDCl_3$, 300 MHz.

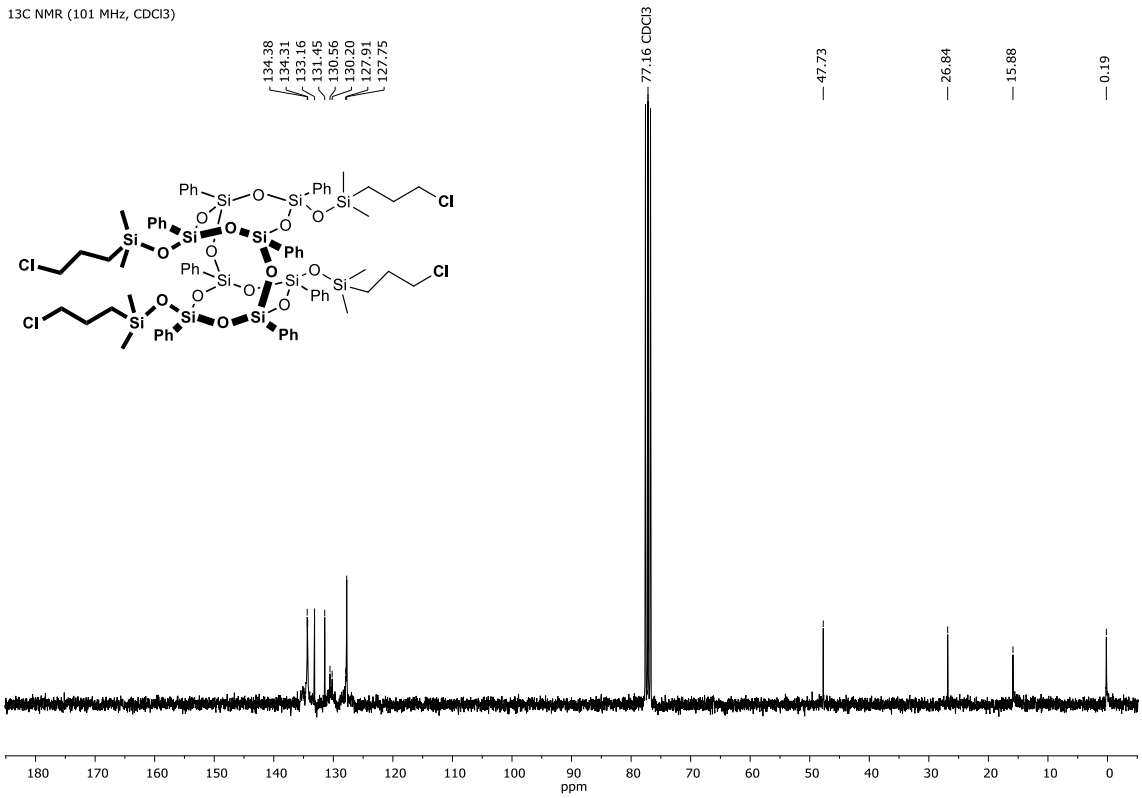

Figure S 3 ^{13}C NMR spectrum of SQ-T1a in $CDCl_3$, 101 MHz.

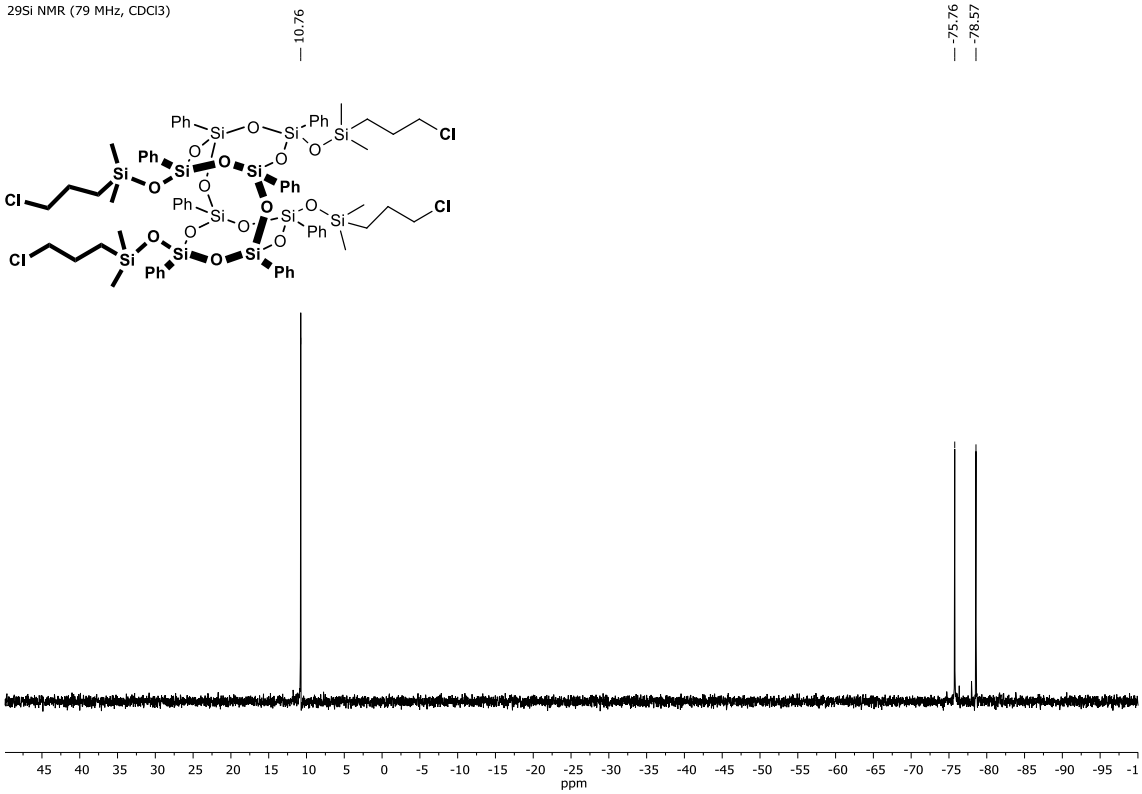

Figure S 4 ^{29}Si NMR spectrum of SQ-T1a in $CDCl_3$, 79 MHz.

SQ-Td1a

Crystalline solid. Isolated Yield 18%.

^{1}H NMR ($CDCl_3$, 300 MHz): δ/ppm = 7.56-7.17 (m, 40H, Ph), 3.42 (t, *J* = 6.9 Hz, 4H), 1.87-1.80 (m, 4H, -CH_2-), 0.78-0.73 (m, 4H, -$SiCH_2$-), 0.26 (s, 12H, -$Si(CH_3)_2$).
^{13}C NMR ($CDCl_3$, 101 MHz): δ/ppm = 134.19, 134.10, 133.05, 130.81, 130.70, 130.55, 127.96, 127.90, 127.73 (Ph), 48.05 (-CH_2-Cl), 26.97 (-CH_2-), 15.85 (-$SiCH_2$-), 0.29 (-$Si(CH_3)_2$).
^{29}Si NMR ($CDCl_3$, 79 MHz): δ/ppm = 11.80 (-$Si(CH_3)_2$), -75.81, -76.31, -77,94.
IR (ATR, cm-1): 3072.51, 3050.60 (C-H phenyl), 3027.69 (=C-H), 2954.06 (C-H), 1593.68, 1429.91 (C=C phenyl), 1253.82 (Si-C), 1063.66 (Si-O-Si), 997.51 (C-H phenyl).
EA: Anal. calcd for $C_{58}H_{64}Cl_2O_{13}Si_{10}$ (%):C, 52.74, H, 4.88; found: C, 52.69; H, 4.93.
ESI-MS: Calcd. for $C_{58}H_{64}Cl_2Na^{+}O_{13}Si_{10}$: *m/z* 1341.1309 [M + Na^{+}]. Found: 1341.1224.

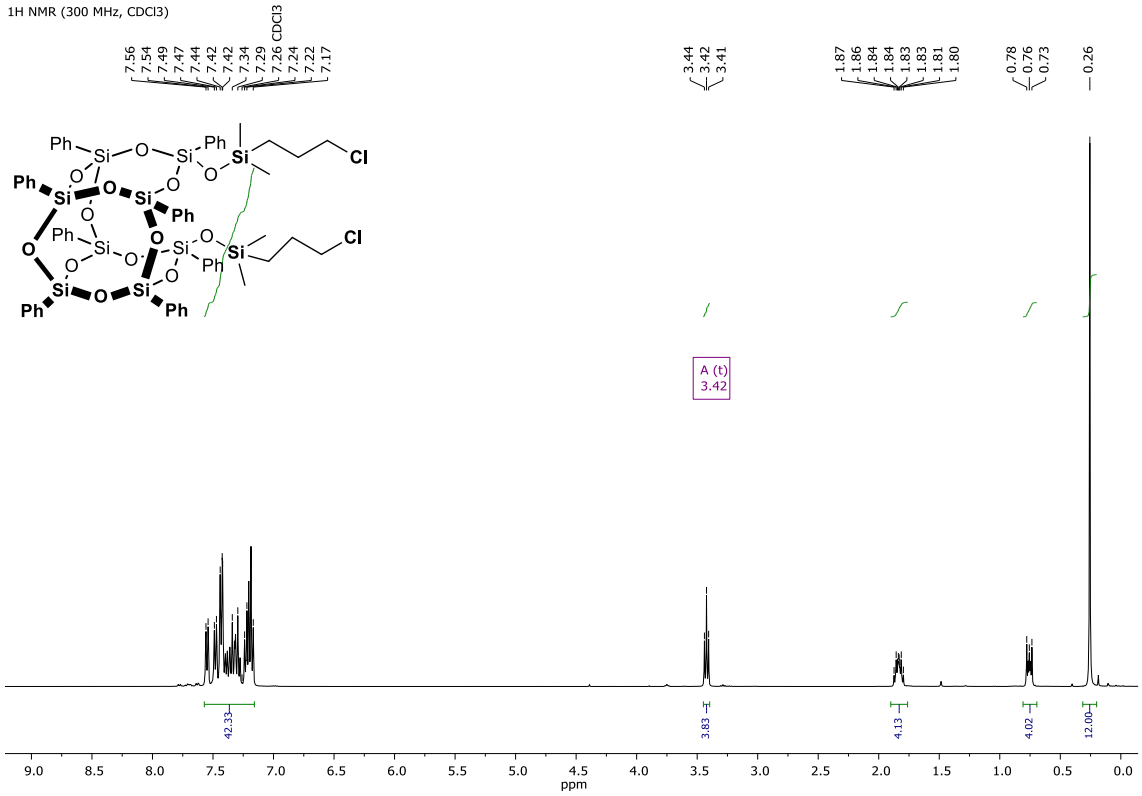

Figure S 5 ^{1}H NMR spectrum of SQ-Td1a in $CDCl_3$, 300 MHz.

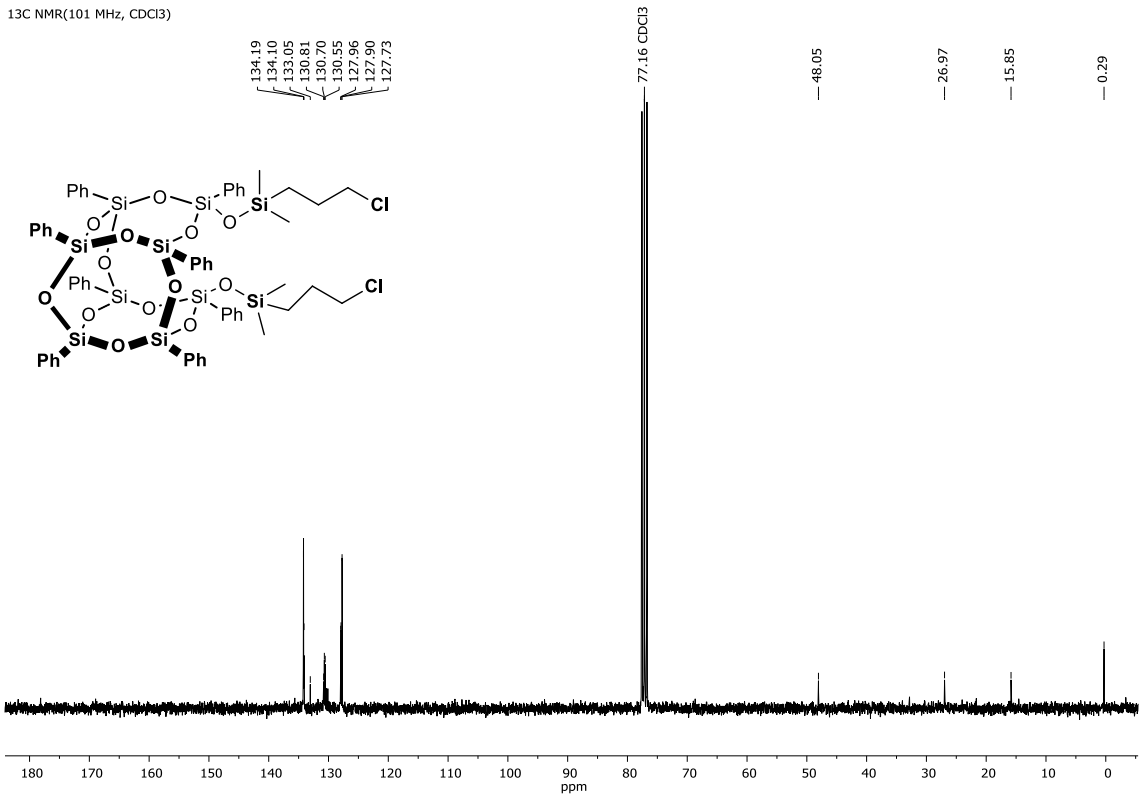

Figure S 6 ^{13}C NMR spectrum of SQ-Td1a in $CDCl_3$, 101 MHz.

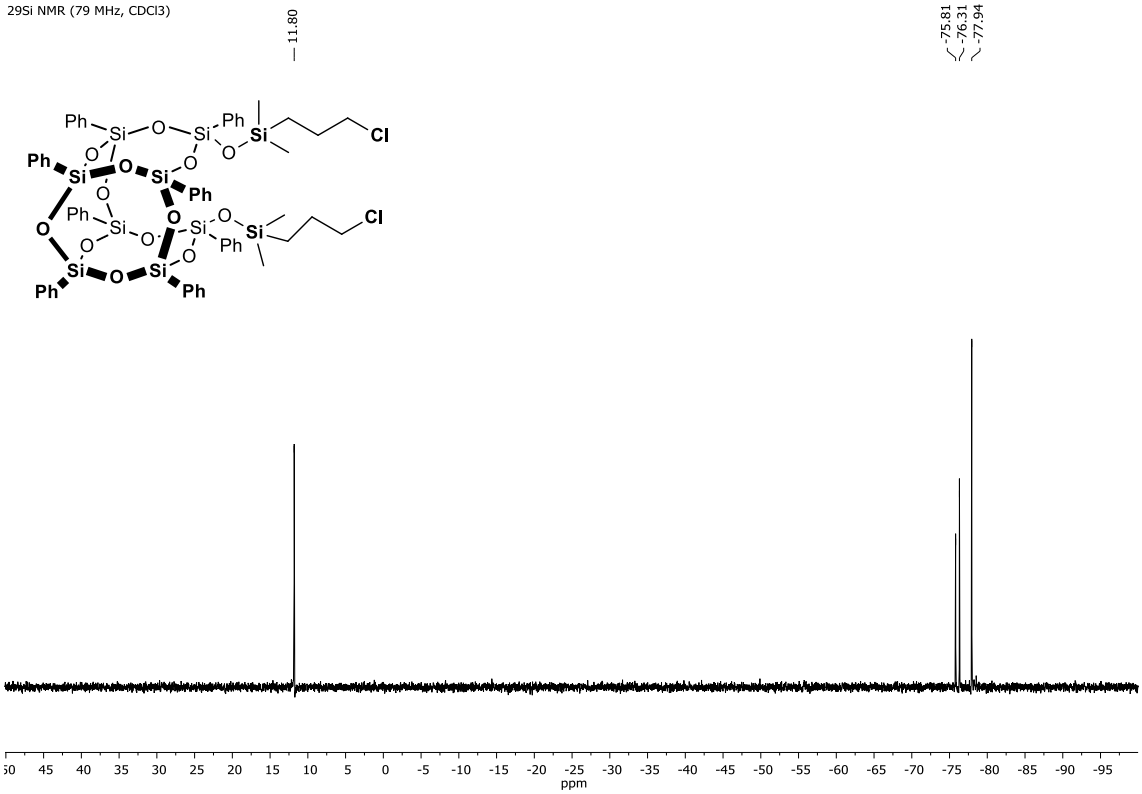

Figure S 7 ^{29}Si NMR spectrum of SQ-Td1a in $CDCl_3$, 79 MHz.

SQ-T1b

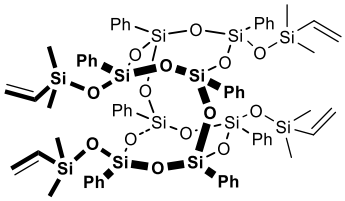

White solid. Isolated Yield 90%.

All analyses including NMR spectra, FT-IR, MALDI-TOF MS and crystal structure were presented previously.[5]

SQ-Td1b

White solid. Isolated Yield 8%.
^{1}H NMR ($CDCl_3$, 300 MHz): δ/ppm = 7.57-7.15 (m, 40H, Ph), 6.21 (dd, $J_{H\text{-}H}$ = 20.3, 14.9 Hz, 2H), 5.97 (dd, $J_{H\text{-}H}$ = 14.9, 3.8 Hz, 2H), 5.832 (dd, $J_{H\text{-}H}$ = 20.2, 3.8 Hz, 2H), 0.30 (s, 12H, -Si(CH_3)$_2$).
^{13}C NMR ($CDCl_3$, 101 MHz): δ/ppm = 138.71 (-CH=CH_2), 134.24, 133.24 (Ph), 132.58 (-CH=CH_2), 130.92, 130.78, 130.44, 130.21, 127.90, 127.84, 127.66 (Ph), 0.47 (-Si(CH_3)$_2$).
^{29}Si NMR ($CDCl_3$, 79 MHz): δ/ppm = 0.21 (-(Vi)Si(CH_3)$_2$), -75.99, -76.37, -78.16.
IR (ATR): 3072.48, 3050.90 (C-H phenyl), 3016.96 (=C-H), 2959.65 (C-H), 1593.80, 1430.05 (C=C phenyl), 1253.39 (Si-C), 1113.95, 1067.01, 1029.18 (Si-O-Si), 998.39 (C-H phenyl).
EA: Anal. Calcd. for $C_{56}H_{58}O_{13}Si_{10}$ (%):C, 55.14, H, 4.79; found: C, 55.19; H, 4.83.
ESI-MS: Calcd. for $C_{56}H_{62}Na^{+}O_{13}Si_{10}$: *m/z* 1236.1908 [M + NH_4]$^{+}$. Found: 1236.1892.

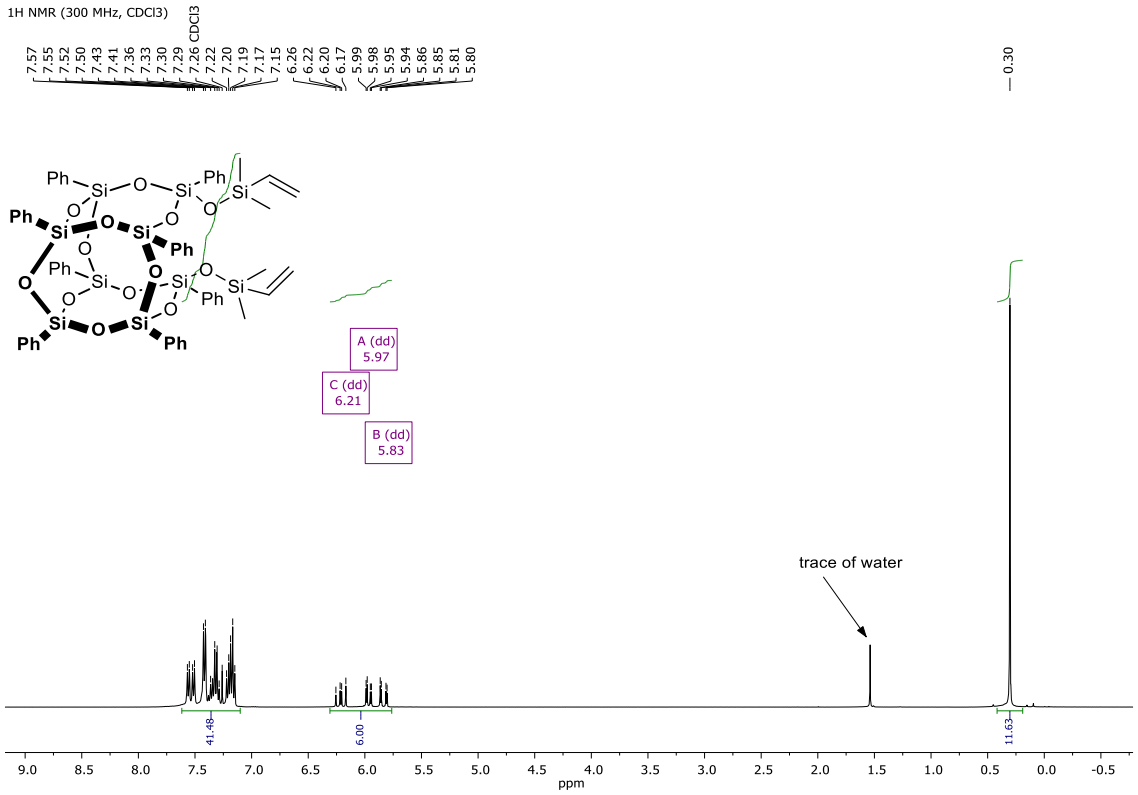

Figure S 8 ^{1}H NMR spectrum of SQ-Td1b in $CDCl_3$, 300 MHz.

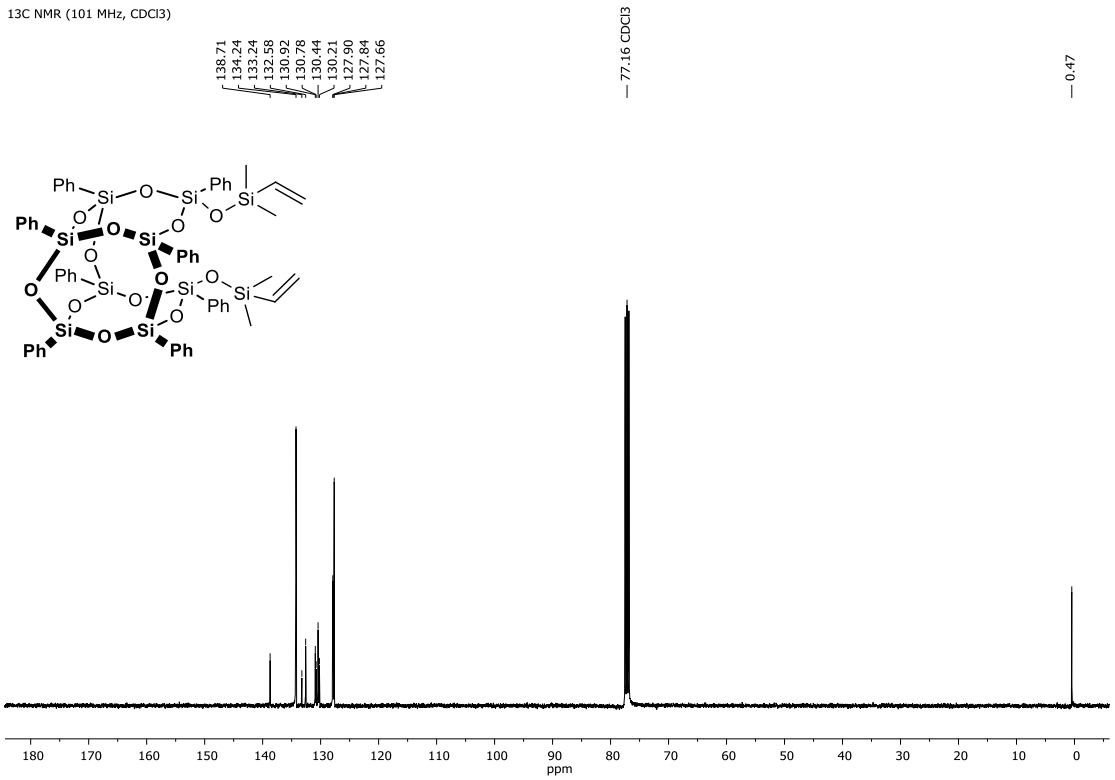

Figure S 9 ^{13}C NMR spectrum of SQ-Td1b in $CDCl_3$, 101 MHz.

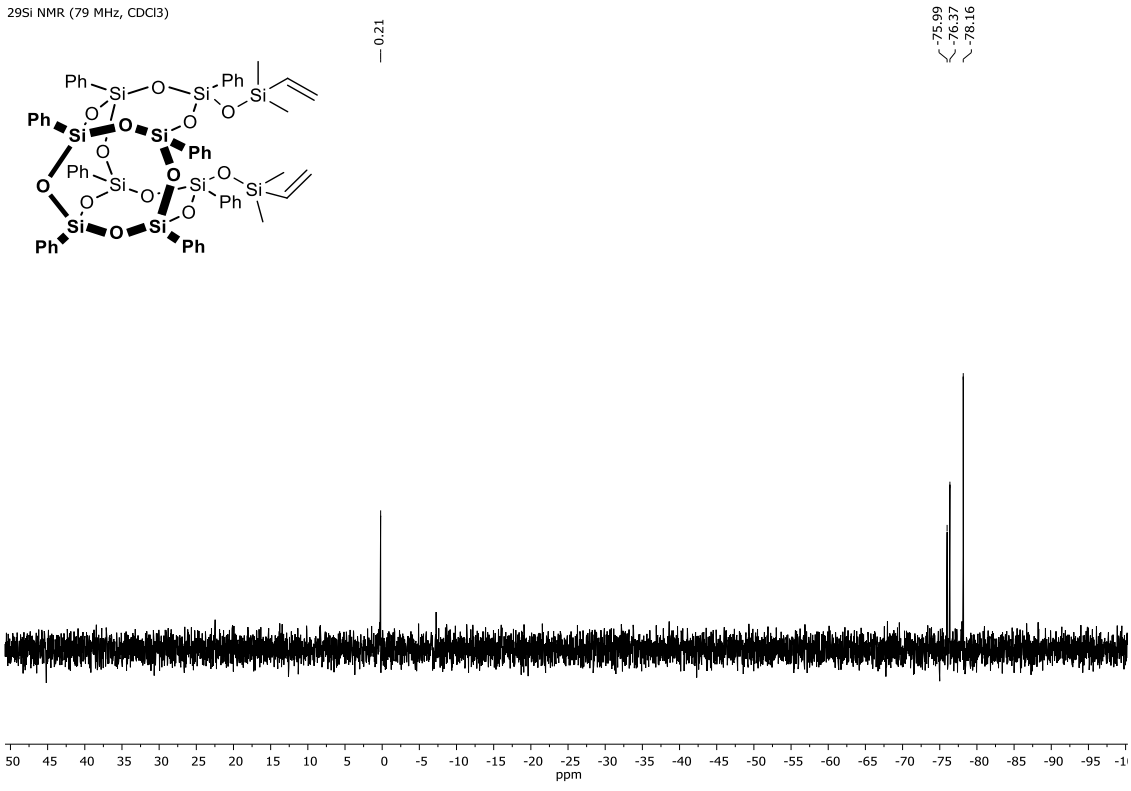

Figure S 10 ^{29}Si NMR spectrum of SQ-Td1b in $CDCl_3$, 79 MHz.

SQ-T1c

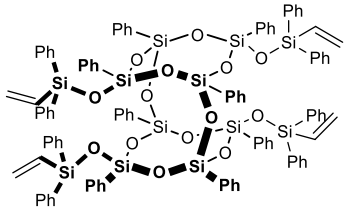

White solid. Isolated Yield 65%.

All analyses including NMR spectra, FT-IR and MALDI-TOF MS were presented previously.[5]

SQ-Td1c

White solid. Isolated Yield 25%.
^{1}H NMR ($CDCl_3$, 300 MHz): δ/ppm = 7.55-7.07 (m, 60H, Ph), 6.31 (dd, $J_{H\text{-}H}$ = 20.1, 14.9 Hz, 2H), 6.08 (dd, $J_{H\text{-}H}$ = 14.8, 3.8 Hz, 2H), 5.87 (dd, $J_{H\text{-}H}$ = 20.1, 3.8 Hz, 2H).
^{13}C NMR ($CDCl_3$, 101 MHz): δ/ppm = 136.85 (-CH=CH_2), 135.16, 134.96, 134.27 (Ph), 132.74 (-CH=CH_2), 130.77, 130.64, 130.40, 130.21, 129.76, 127.87, 127.76, 127.58 (Ph).
^{29}Si NMR ($CDCl_3$, 79 MHz): δ/ppm = -20.30 (-Si(Ph)$_2$-Vi), -75.30, -76.18, -77.72.
IR (ATR): 3070.96, 3052.73 (C-H phenyl), 3007.01 (=C-H), 1593.59, 1429.26 (C=C phenyl), 1130.41, 1108.24 1072.59, 1028.00 (Si-O-Si), 997.87 (C-H phenyl).
ESI-MS: Calcd. for $C_{76}H_{70}Na^{+}O_{13}Si_{10}$: *m/z* 1484.2534 [M + NH_4^+]. Found: 1484.2534.

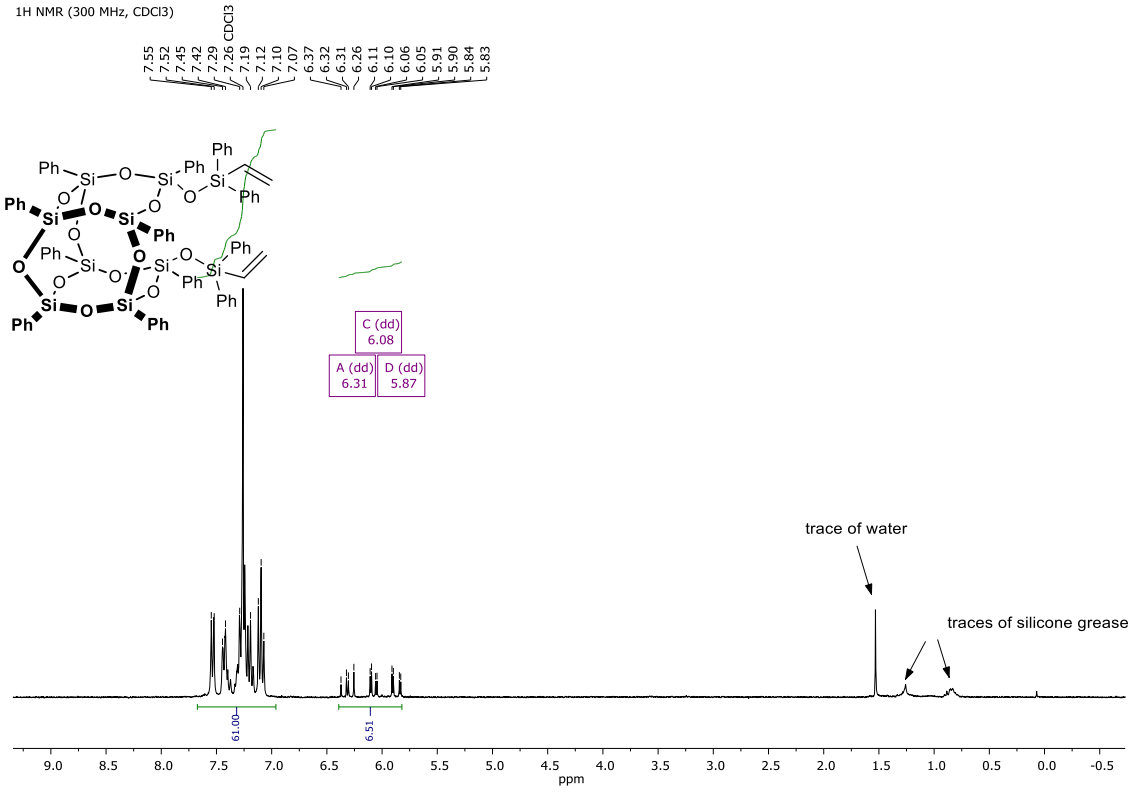

Figure S 11 ^{1}H NMR spectrum of SQ-Td1c in $CDCl_3$, 300 MHz.

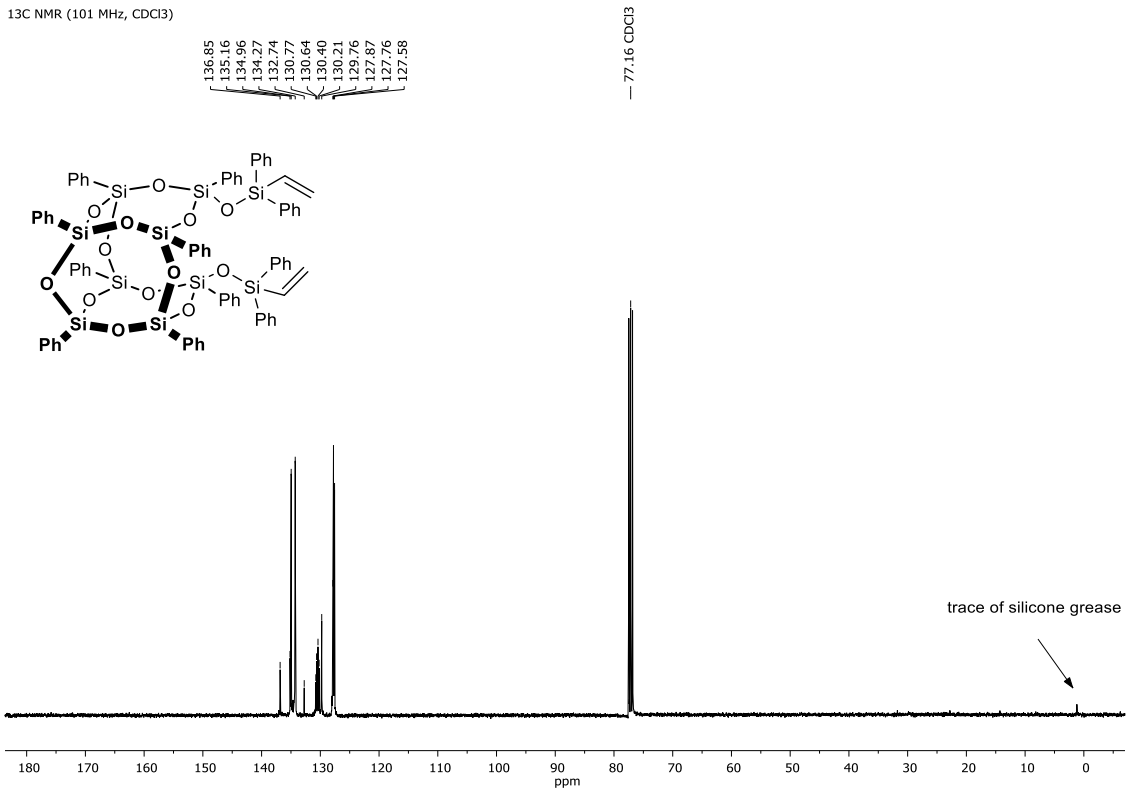

Figure S 12 ^{13}C NMR spectrum of SQ-Td1c in $CDCl_3$, 101 MHz.

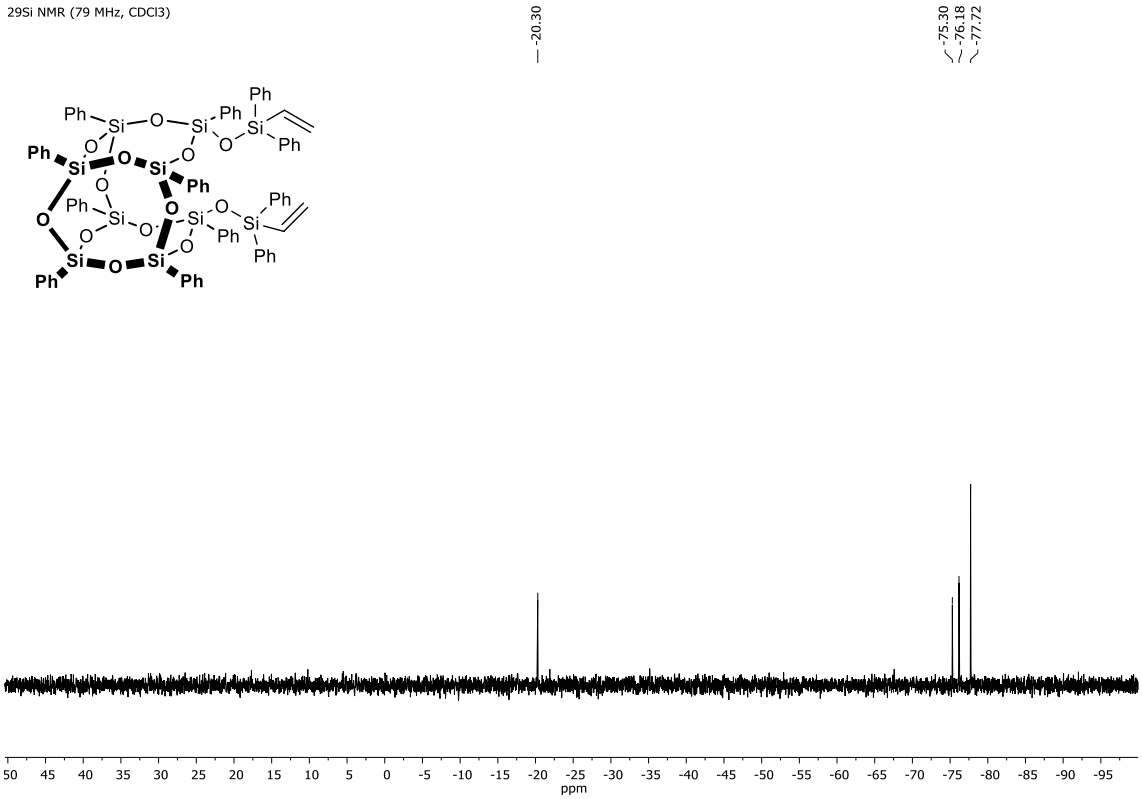

Figure S 13 ^{29}Si NMR spectrum of SQ-Td1c in $CDCl_3$, 79 MHz.

SQ-T1d

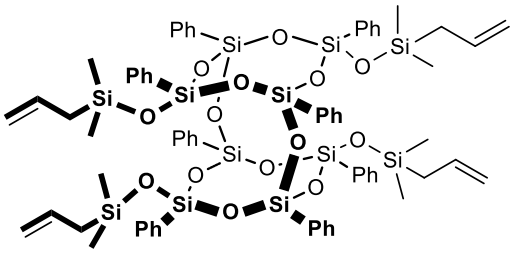

Crystal solid. Isolated Yield 69%.

All analyses including NMR spectra, FT-IR and MALDI-TOF MS were presented previously. [5] However in this paper We present crystal structure.

Picture S 1 Microscope photo of SQ-T1d.

Picture S 2 Microscope photo of SQ-T1d.

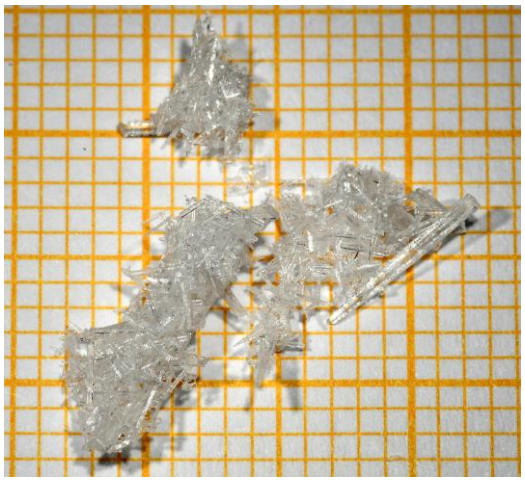

Picture S 3 Microscope photo of SQ-T1d presented on mm paper.

SQ-Td1d

Picture S 4 Microscope photo of SQ-Td1d presented on mm paper.

White solid. Isolated Yield 15%.

^{1}H NMR ($CDCl_3$, 300 MHz): δ/ppm = 7.56-7.18 (m, 40H, Ph), 5.90-5.75 (m, 2H, CH=), 4.91-4.81 (m, 4H $=CH_2$), 1.70 (d, $J_{H\text{-}H}$ = 8.1 Hz, 4H, $-CH_2-$), 0.25 (s, 12H, $-Si(CH_3)_2$).
^{13}C NMR ($CDCl_3$, 101 MHz): δ/ppm = 134.23-134.19, 133.21 (Ph), 130.87 ($-CH=CH_2$), 130.79 (Ph), 130.48, 130.25, 127.90-127.69 (Ph), 113.86 ($-CH=CH_2$), 26.12 ($-CH_2-$), -0.12 ($-Si(CH_3)_2$).
^{29}Si NMR ($CDCl_3$, 79 MHz): δ/ppm = 8.92 ($-(All)Si(CH_3)_2$), -76.04, -76.34, -78.05.
IR (ATR): 3072.88, 3051.27 (C-H phenyl), 3028.09 (=C-H), 2959.19 (-C-H), 1629.97 (C=C), 1594.15, 1429.91 (C=C phenyl), 1255.93 (Si-C), 1050.68, 1026.91 (Si-O-Si), 996.99 (C-H phenyl).
EA: Anal. calcd for $C_{58}H_{62}O_{13}Si_{10}$ (%):C, 55.82, H, 5.01; found: C, 55.89; H, 5.03.
ESI-MS: Calcd. for $C_{58}H_{62}Na^{+}O_{13}Si_{10}$: *m/z* 1269.1775 [M + Na^{+}]. Found: 1269.1775.

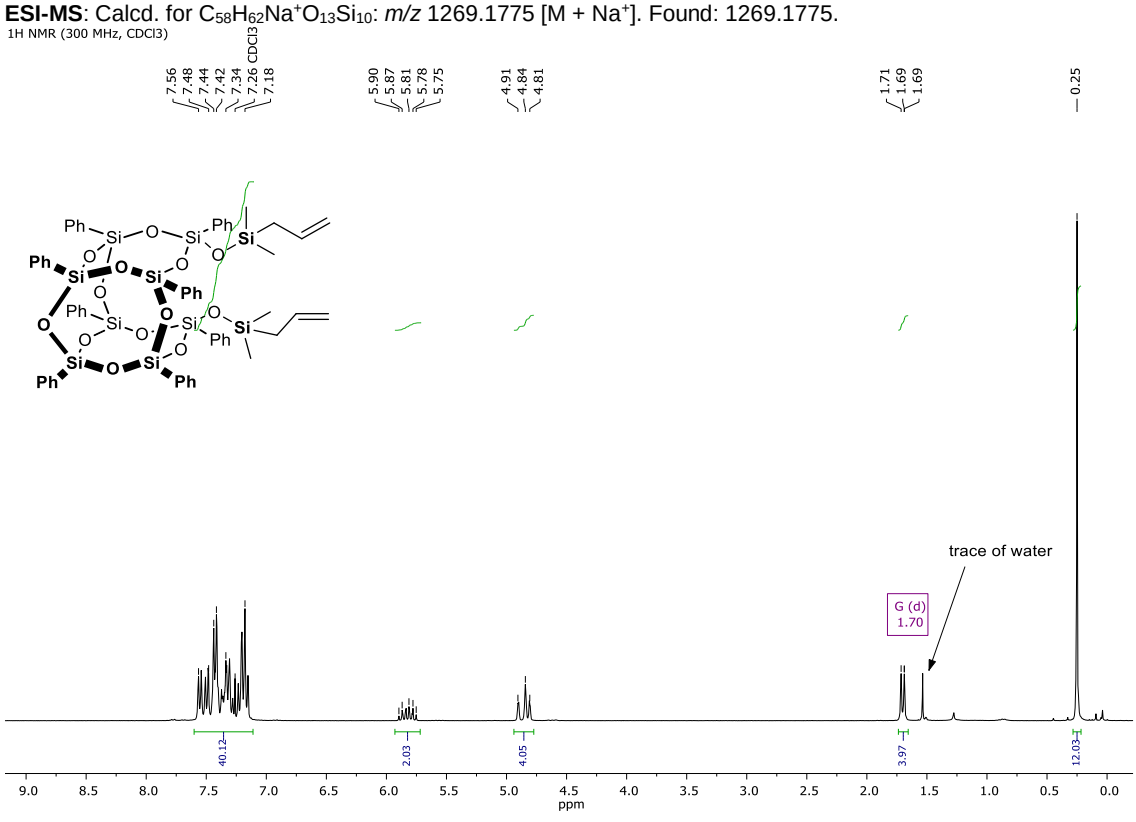

Figure S 14 ^{1}H NMR spectrum of SQ-Td1d in $CDCl_3$, 300 MHz.

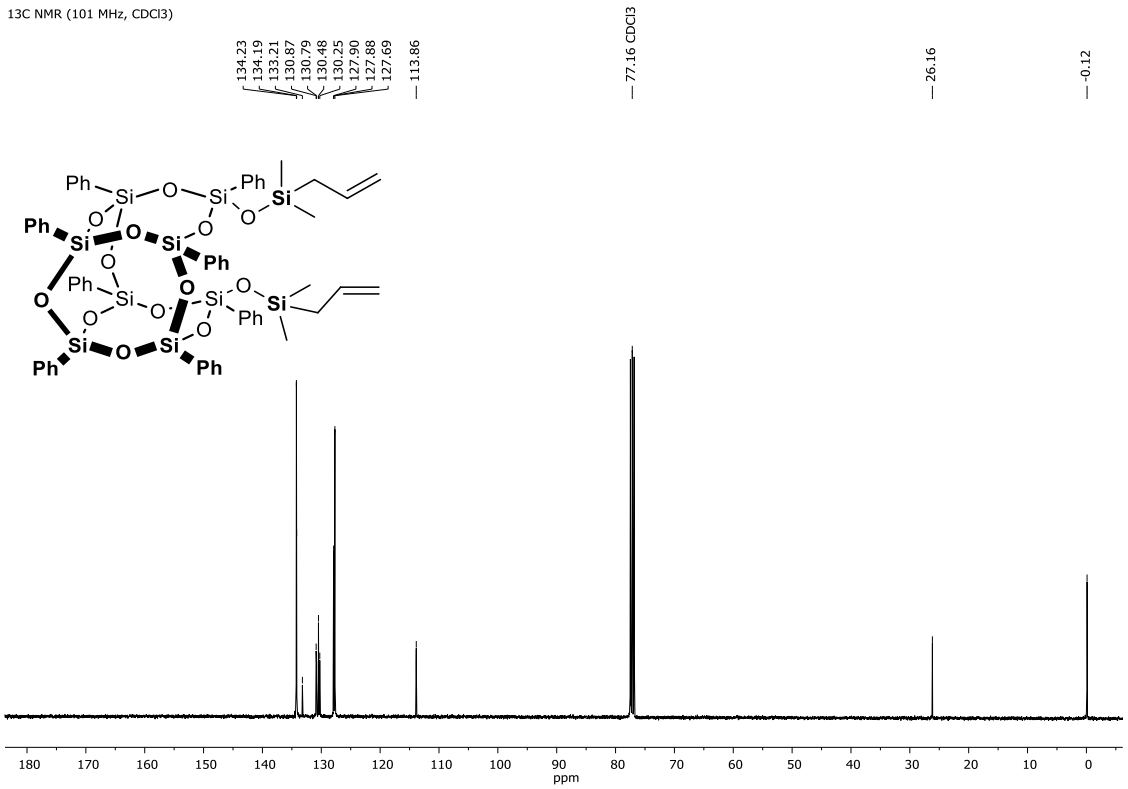

Figure S 15 ^{13}C NMR spectrum of SQ-Td1d in $CDCl_3$, 101 MHz.

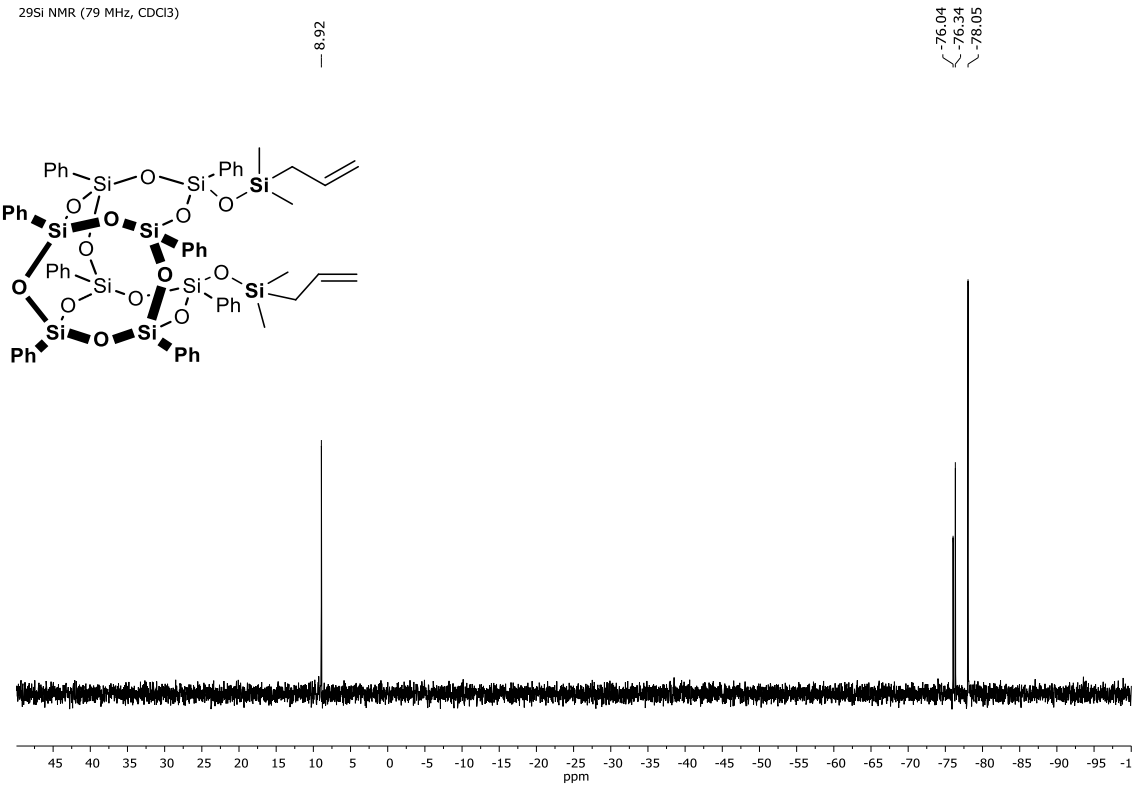

Figure S 16 ^{29}Si NMR spectrum of SQ-Td1d in $CDCl_3$, 79 MHz.

SQ-D2a

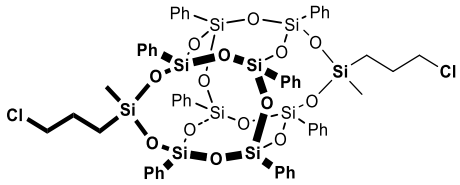

White solid. Isolated Yield 70%.

Analytical data (NMR spectra, FT-IR and MALDI-TOF MS) correspond with the literature.[6]

SQ-Dm2a

Crystal solid. Isolated Yield 15%.

^{1}H NMR ($CDCl_3$, 300 MHz): δ/ppm = 7.74-7.72 (m, 40H, Ph), 3.45-3.41 (t, 2H, -CH_2-Cl), 1.93-1.83 (m, 2H, -CH_2-), 0.88-0.83 (m, 2H, -$SiCH_2$-), 0.33 (s, 3H, -$SiCH_3$).
^{13}C NMR ($CDCl_3$, 101 MHz): δ/ppm = 134.33, 134.26, 133.99, 131.90, 130.91, 130.78, 130.61, 130.41 128.03, 127.93 (Ph), 47.59 (-CH_2-Cl), 26.53 (-CH_2-), 14.51 (-$SiCH_2$-), -0.73 (-$SiCH_3$).
^{29}Si NMR ($CDCl_3$, 79 MHz): δ/ppm = -18.79 (-$SiCH_3$), -77.40, -78.83, -78.88, -79.19.
IR (ATR, cm^{-1}): 3072.41, 3050.63 (C-H phenyl), 3027.52 (=C-H), 2954.57 (-C-H), 1594.21, 1430.04 (C=C phenyl), 1263.02 (Si-C), 1083.75, 1028.80 (Si-O-Si), 997.98 (C-H phenyl).
EA: Anal. calcd for $C_{52}H_{49}ClO_{13}Si_9$ (%):C, 53.37, H, 4.22; found: C, 54.62; H, 4.65.
ESI-MS: Calcd. for $C_{52}H_{49}ClNa^{+}O_{13}Si_9$: *m/z* 1191.0677 [M + Na^{+}]. Found: 1191.0788.

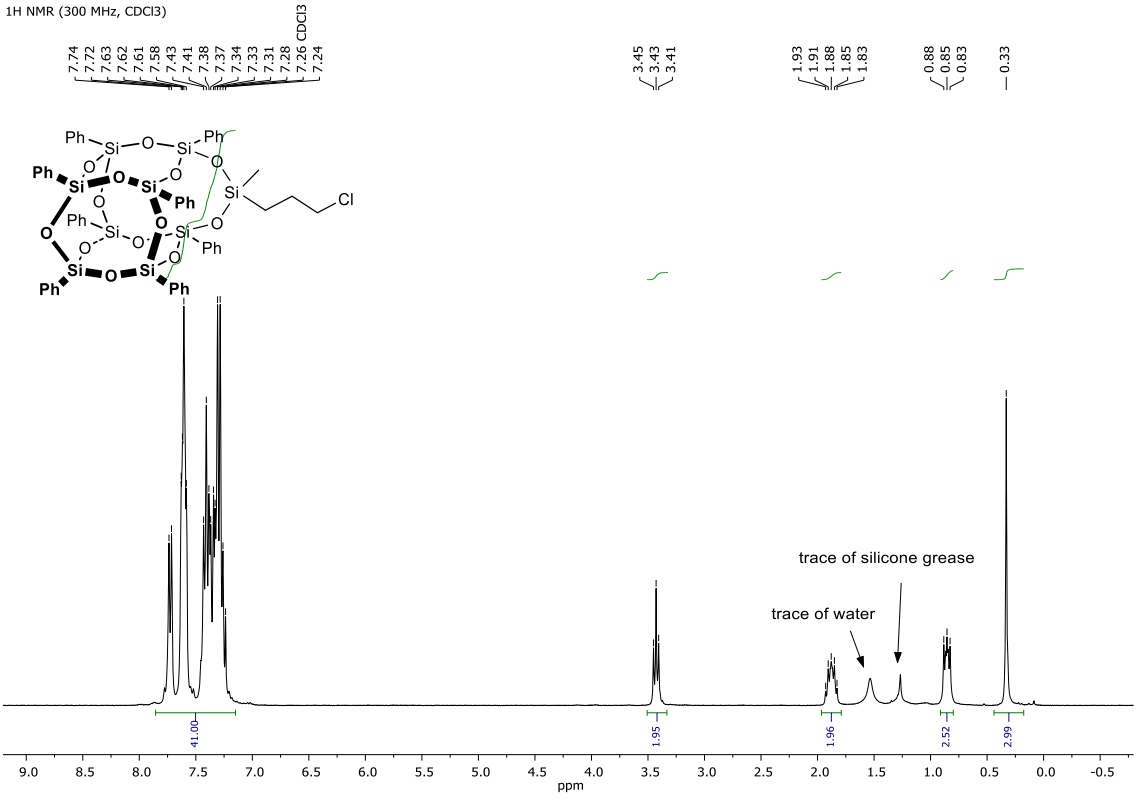

Figure S 17 ^{1}H NMR spectrum of SQ-Dm2a in $CDCl_3$, 300 MHz.

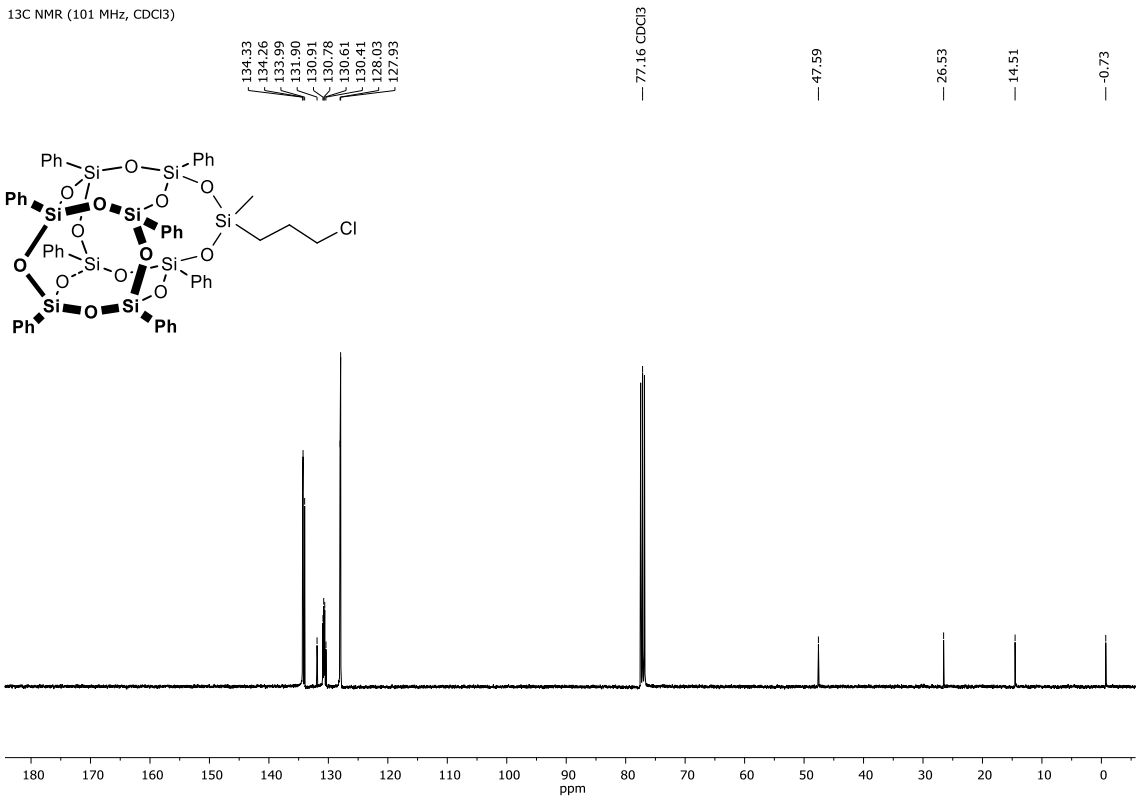

Figure S 18 ^{13}C NMR spectrum of SQ-Dm2a in $CDCl_3$, 101 MHz.

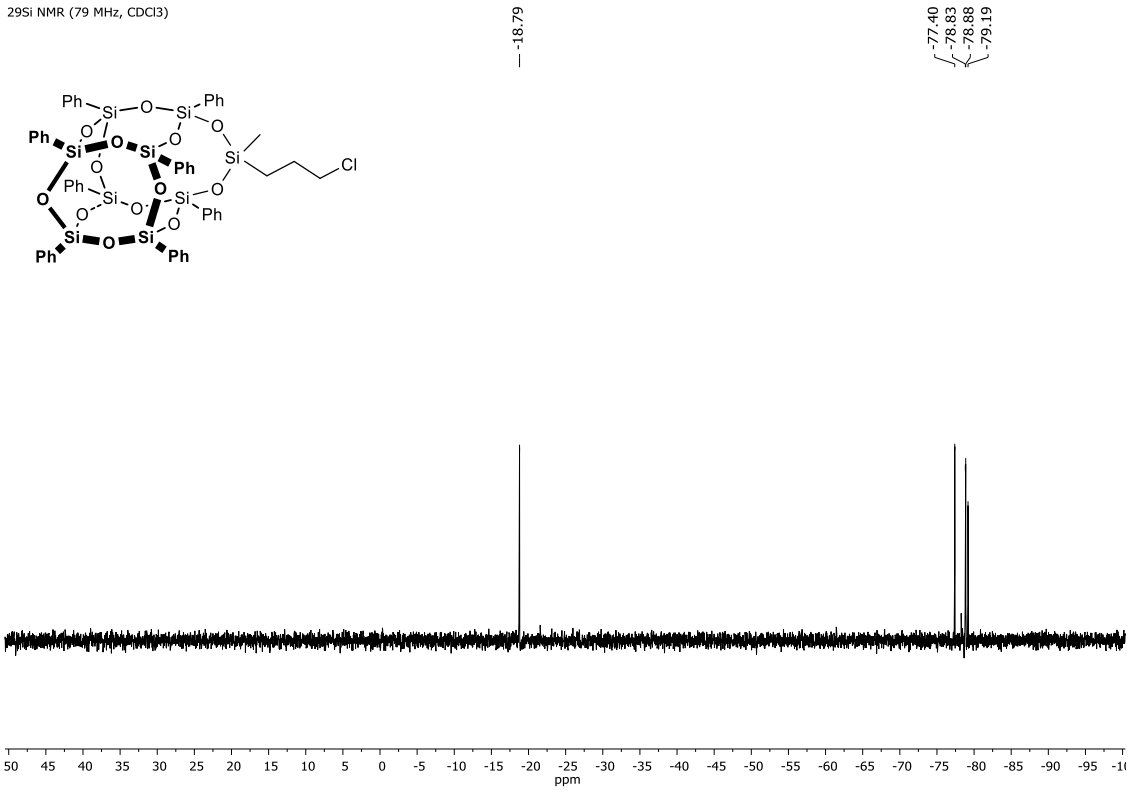

Figure S 19 ^{29}Si NMR spectrum of SQ-Dm2a in $CDCl_3$, 79 MHz.

SQ-D2b

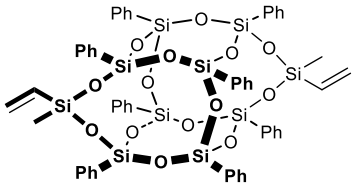

White solid. Isolated Yield 78%.

All analyses including NMR spectra, FT-IR, MALDI-TOF MS and crystal structure were presented previously.[7]

SQ-Dm2b

Crystal solid. Isolated Yield 6%.

^{1}H NMR ($CDCl_3$, 300 MHz): δ/ppm = 7.74-7.25 (m, 40H, Ph), 6.18 (dd, J_{H-H} = 19.6, 15.1 Hz, 1H), 6.02 (dd, J_{H-H} = 15.0, 4.3 Hz, 1H), 5.94 (dd, J_{H-H} = 19.7, 4.3 Hz, 1H), 0.39 (s, 3H, -$SiCH_3$).
^{13}C NMR ($CDCl_3$, 101 MHz): δ/ppm = 135.40 (-CH=CH2), 134.53, 134.07, 134.33 (Ph), 131.96 (-CH=CH2), 130.48, 130.88, 127.87, 127.99 (Ph), -0.97 (-$SiCH_3$).
^{29}Si NMR ($CDCl_3$, 79 MHz): δ/ppm = -31.88 (-(Vi)$Si(CH_3)$), -77.45, -78.96, -79.11.
IR (ATR): 3072.47, 3051.05 (C-H phenyl), 3027.41 (=C-H), 1594.46, 1430.11 (C=C phenyl), 1264.95 (Si-C), 1086.86, 1028.56 (Si-O-Si), 997.70 (C-H phenyl).
EA: Anal. calcd for $C_{51}H_{46}O_{13}Si_9$ (%):C, 54.71, H, 4.14; found: C, 54.79; H, 4.23.
ESI-MS: Calcd. for $C_{51}H_{50}Na^{+}O_{13}Si_9$: *m/z* 1136.1200 [M + NH_4^{+}]. Found: 1136.1191.

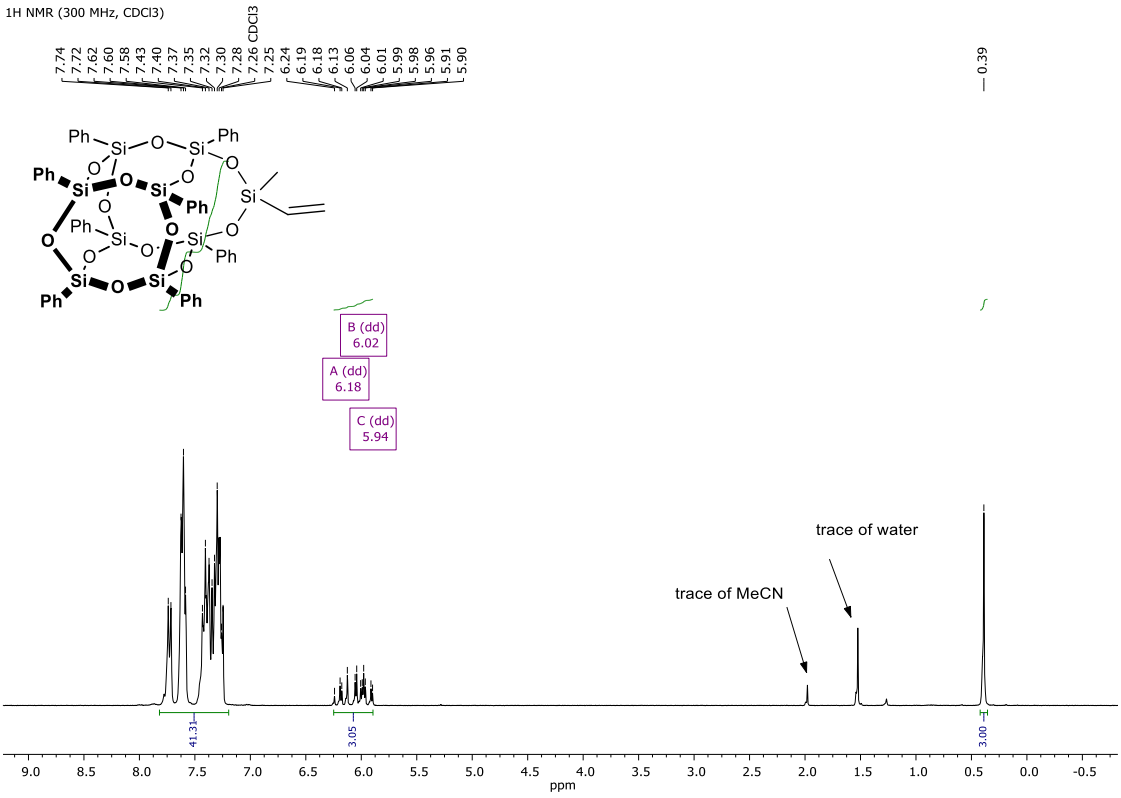

Figure S 20 ^{1}H NMR spectrum of SQ-Dm2b in $CDCl_3$, 300 MHz.

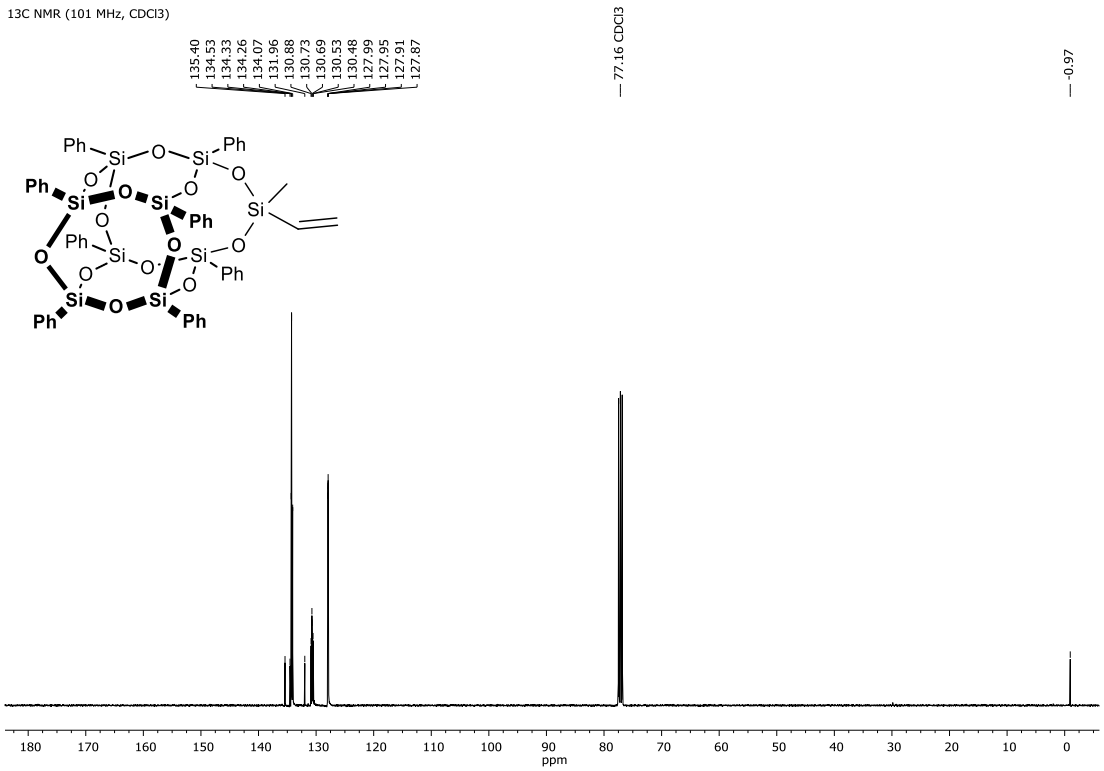

Figure S 21 ^{13}C NMR spectrum of SQ-Dm2b in $CDCl_3$, 101 MHz.

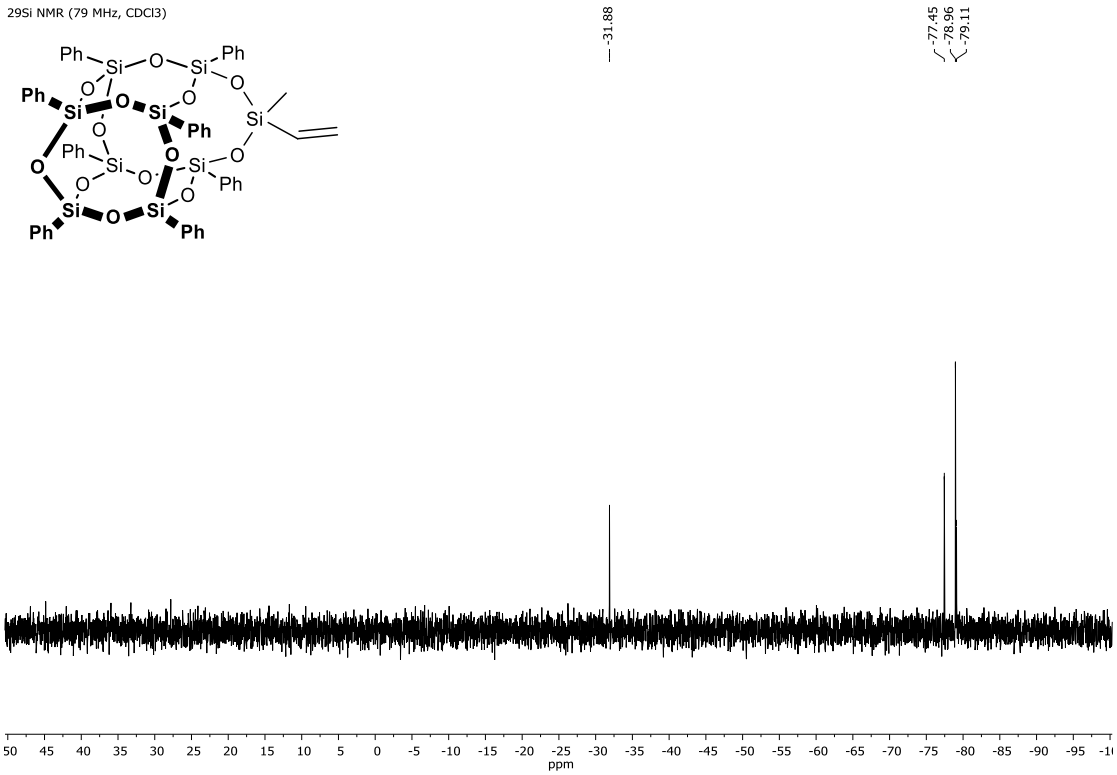

Figure S 22 ^{29}Si NMR spectrum of SQ-Dm2b in $CDCl_3$, 79 MHz.

SQ-D2d

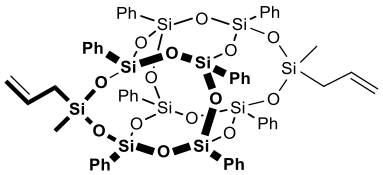

Crystal solid. Isolated Yield 70%.

Spectroscopy analyses, including NMR and FT-IR, were presented previously.[8]

EA: Anal. calcd for $C_{56}H_{56}O_{14}Si_{10}$ (%):C, 54.51, H, 4.57; found: C, 54.62; H, 4.65.
ESI-MS: Calcd. for $C_{56}H_{56}Na^{+}O_{14}Si_{10}$: *m/z* 1255.1255 [M + Na^{+}]. Found: 1255.1254.

SQ-Dm2d

White solid. Isolated Yield 12%.
^{1}H NMR ($CDCl_3$, 300 MHz): δ/ppm = 7.74-7.26 (m, 40H, Ph), 5.86-5.72 (m, 1H, -CH=), 4.91-4.77 (m, 2H =CH_2), 1.80 (d, $J_{H\text{-}H}$ = 8.0 Hz, 2H, -CH_2-), 0.33 (s, 3H, -$SiCH_3$).
^{13}C NMR ($CDCl_3$, 101 MHz): δ/ppm = 134.33, 134.25, 134.08, 132.86 (Ph), 131.94 (-CH=CH_2), 130.89, 130.72, 130.45, 128.00. 127.91 (Ph), 114.96 (-CH=CH_2), 24.73 (-CH_2-), -1.49 (-$SiCH_3$).
^{29}Si NMR ($CDCl_3$, 79 MHz): δ/ppm = -22.52 (-(All)Si(CH_3)), -77.46, -78.96, -78.99, -79.35.
IR (ATR): 3072.65, 3050.10 (C-H phenyl), 3024.06 (=C-H), 2961.54, 2923.54 (C-H), 1594.07, 1429.89 (C=C phenyl), 1263.24 (Si-C), 1075.95, 1027.73 (Si-O-Si), 996.87 (C-H phenyl).
EA: Anal. calcd for $C_{52}H_{48}O_{13}Si_9$ (%):C, 55.09, H, 4.27; found: C, 55.12; H, 4.30.
ESI-MS: Calcd. for $C_{52}H_{48}Na^{+}O_{13}Si_9$: *m/z* 1155.0911 [M + Na^{+}]. Found: 1155.0910.

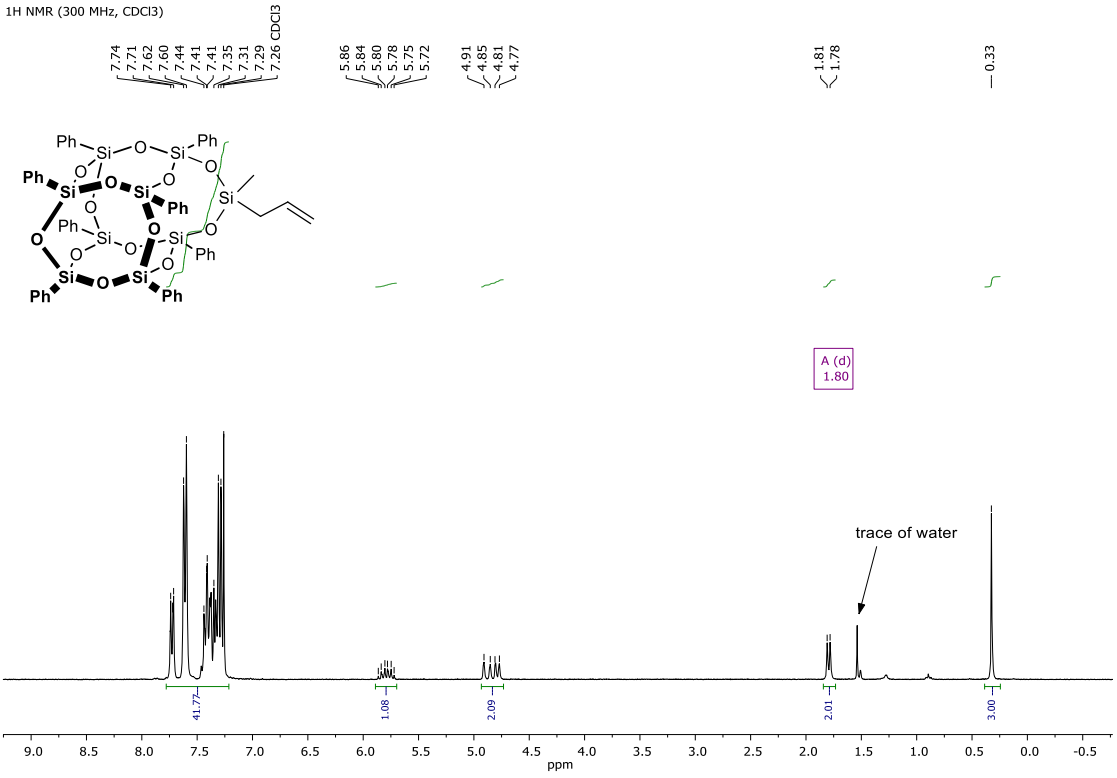

Figure S 23 ^{1}H NMR spectrum of SQ-Dm2d in $CDCl_3$, 300 MHz.

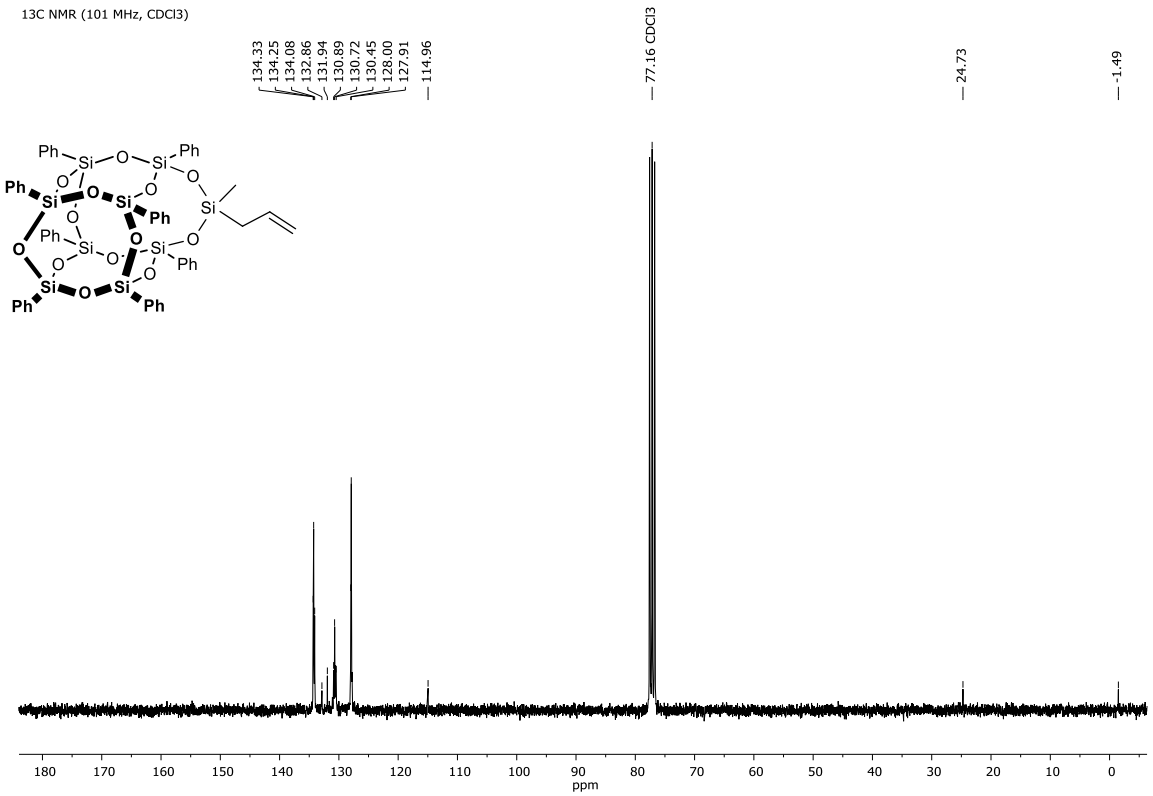

Figure S 24 ^{13}C NMR spectrum of SQ-Dm2d in $CDCl_3$, 101 MHz.

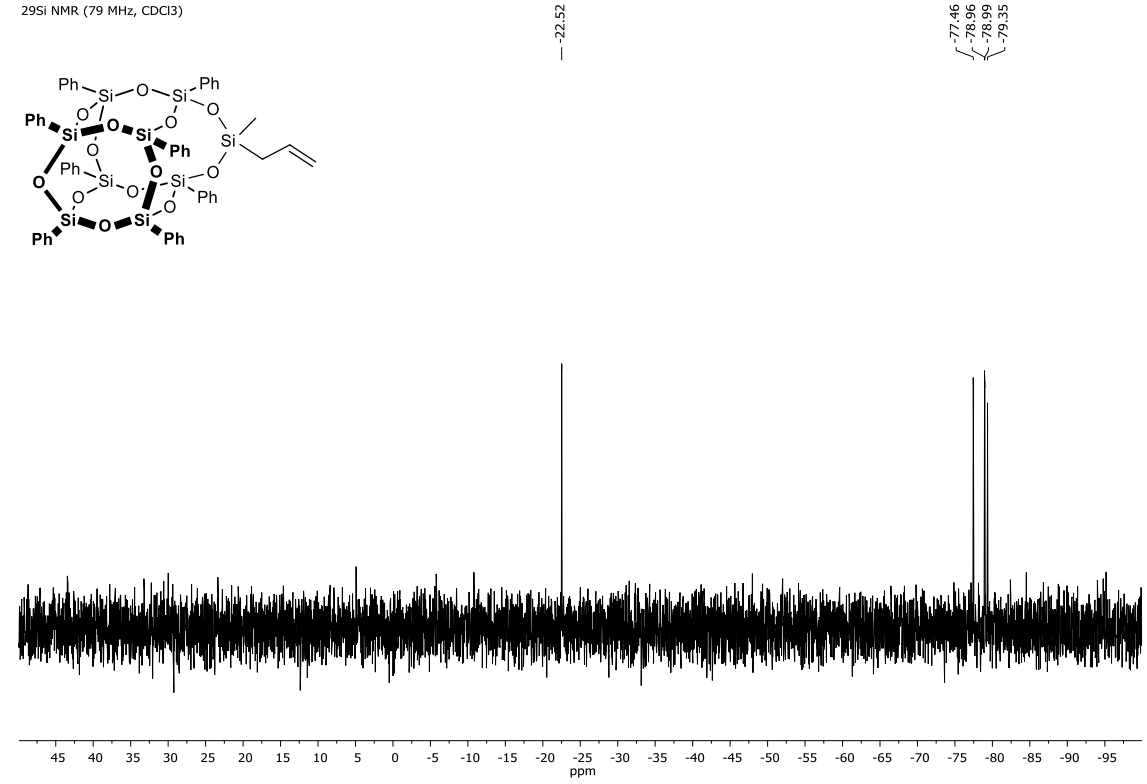

Figure S 25 ^{29}Si NMR spectrum of SQ-Dm2d in $CDCl_3$, 79 MHz.

4.1. Silylative coupling of SQ-T1b with styrene- Postreaction mixture

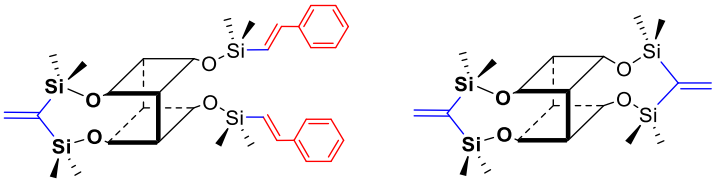

Homo-Hetero coupled product (HHCP) **Homo coupled product (HCP)- SQ-T1b-SC**

White solid.
^{1}H NMR (300 MHz, $CDCl_3$): δ/ppm = 7.44-6.96 (m, Ph), 6.81 (d, J = 19.4 Hz, HHCP), 6.39 (d, J = 19.4 Hz, HHCP), 6.25 (s, $=CH_2$, HCP), 6.21 (s, $=CH_2$, HHCP), 0.25 (s, $-Si(CH_3)_2$, HHCP), 0.23 (s, $-Si(CH_3)_2$, HCP), 0.13 (s, $-Si(CH_3)_2$, HHCP).
^{13}C NMR (101 MHz, $CDCl_3$): δ/ppm = 155.38 ($-C=CH_2$), 144.61 ($-C=CH_2$), 140.36, 138.17, 134.27, 133.23, 131.80, 130.16, 129.94, 128.41, 127.61, 126.74, 0.93 ($-Si(CH_3)_2$, HCP), 0.87 ($-Si(CH_3)_2$, HHCP), 0.82 ($-Si(CH_3)_2$, HHCP).
^{29}Si NMR (79 MHz, $CDCl_3$): δ/ppm = 2.65 ($-Si(CH_3)_2$, HCP), 1.79 ($-Si(CH_3)_2$, HHCP), 0.54 ($-Si(CH_3)_2$, HHCP), -75.81, -78.29, -78.50, -79.45, -80.27.
Homo-hetero-coupledproduct: ESI-MS: Calcd. for $C_{74}H_{80}Na^{+}O_{14}Si_{12}$: *m/z* 1551.2671 $[M + Na]^{+}$. Found: 1551.2693
Homo-coupled product (SQ-T1b-SC): ESI-MS: Calcd. for $C_{60}H_{68}Na^{+}O_{14}Si_{12}$: *m/z* 1371.11732 $[M + Na]^{+}$. Found: 1371.1751

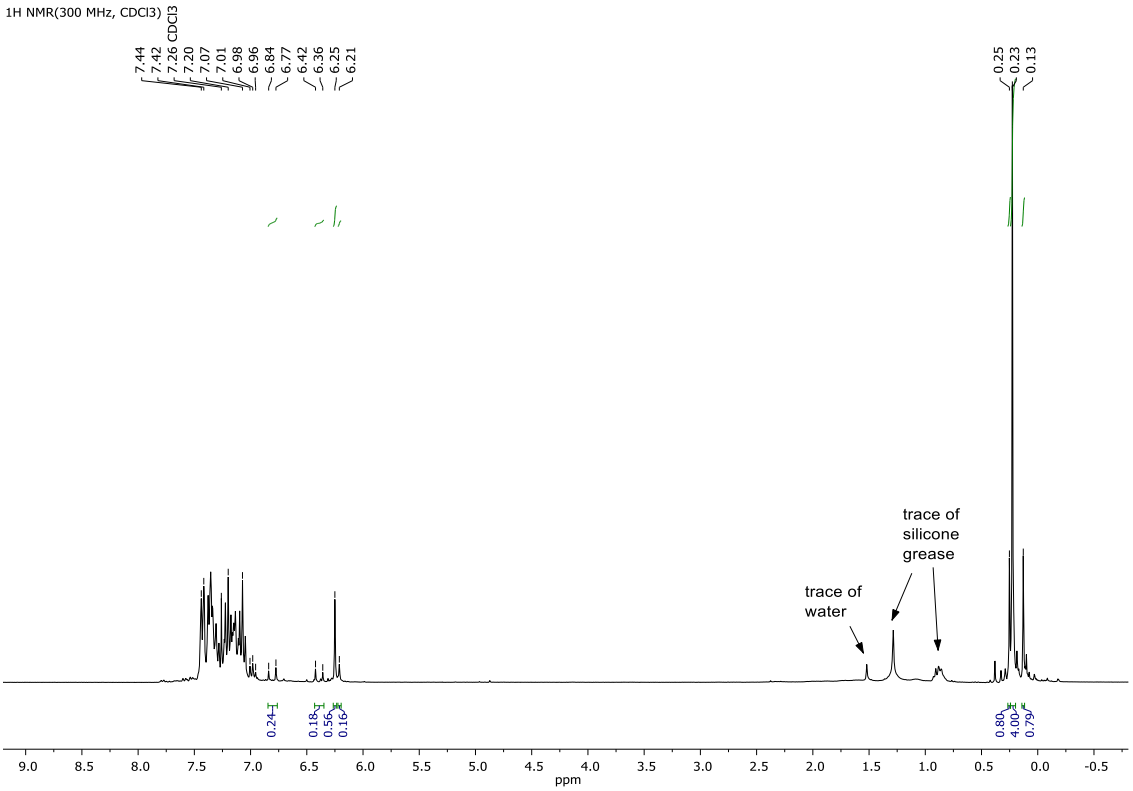

Figure S 26 ^{1}H NMR spectrum of mixture after SC SQ-T1b in $CDCl_3$, 300 MHz.

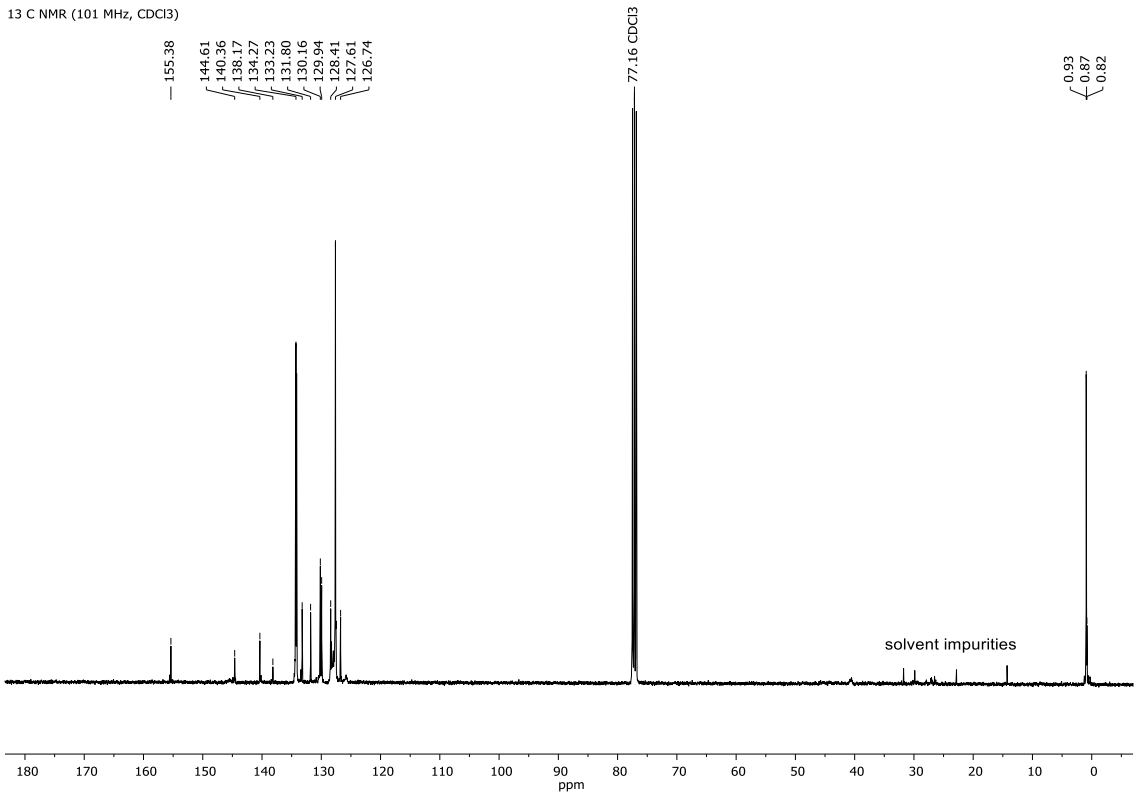

Figure S 27 ^{13}C NMR spectrum of mixture after SC SQ-T1b in $CDCl_3$, 101 MHz.

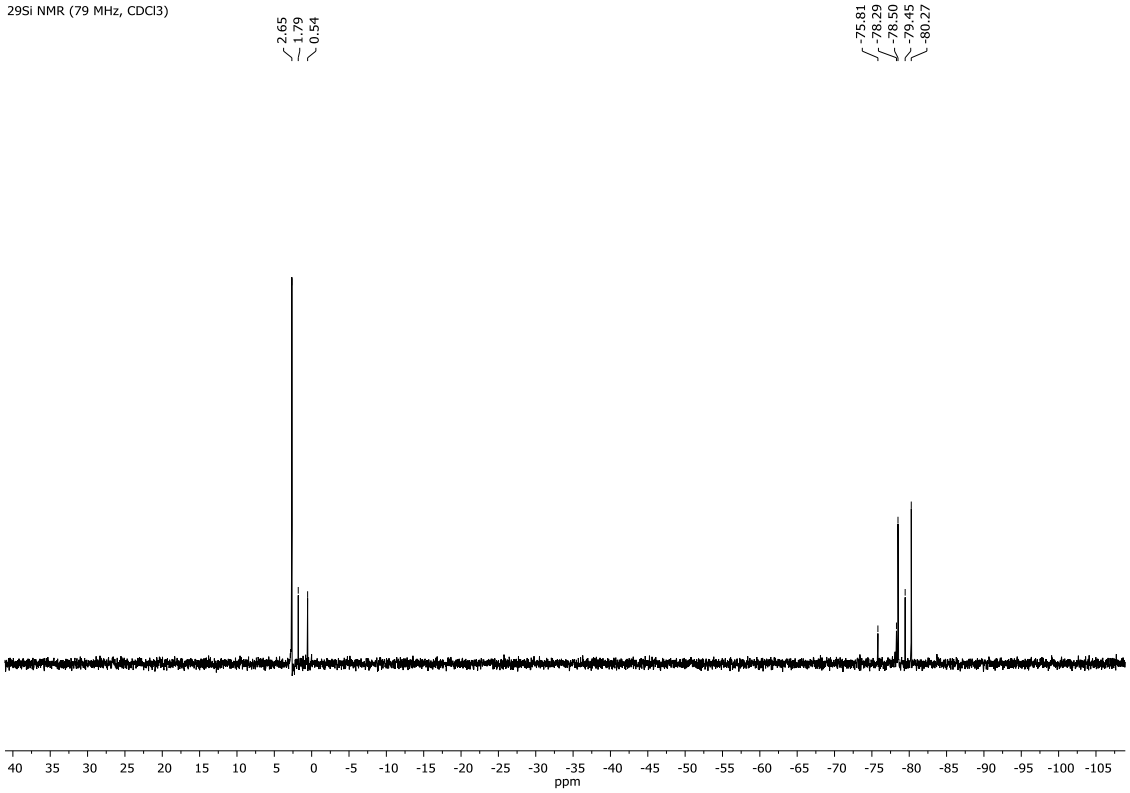

Figure S 28 ^{29}Si NMR spectrum of mixture after SC SQ-T1b in $CDCl_3$.

4.2 Silylative coupling of SQ-Td1c with styrene- Postreaction mixture

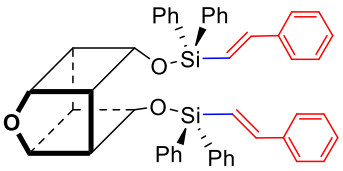

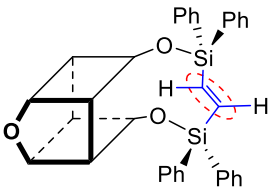

Hetero coupled product (HCP) **Homo coupled product (HCP)- SQ-Td1c-SC**

White solid.

^{1}H NMR ($CDCl_3$, 300 MHz): δ/ppm = 7.66-7.04 (m, Ph), 6.90 (d, J = 19.2 Hz), 6.54 (d, J = 19.2 Hz).

^{13}C NMR ($CDCl_3$, 101 MHz): δ/ppm = 150.17, 148.46, 137.92, 135.21, 135.02, 134.27, 132.84, 132.37, 130.56, 130.45, 130.31, 130.19, 130.02, 129.78, 128.39, 127.96, 127.81, 127.57, 127.07, 123.80.

^{29}Si NMR ($CDCl_3$, 79 MHz): δ/ppm = -19.06 (HCP), -21.91 (HCP), -74.91, -76.16, -76.24, -77.65, -78.06.

HOMO: ESI-MS: Calcd. for $C_{74}H_{62}Na^{+}O_{13}Si_{10}$: *m/z* 1461.1775 [M + Na]$^{+}$. Found: 1461.1777.

HETERO: ESI-MS: Calcd. for $C_{88}H_{74}Na^{+}O_{13}Si_{10}$: *m/z* 1641.2714 [M + Na]$^{+}$. Found: 1641.2760.

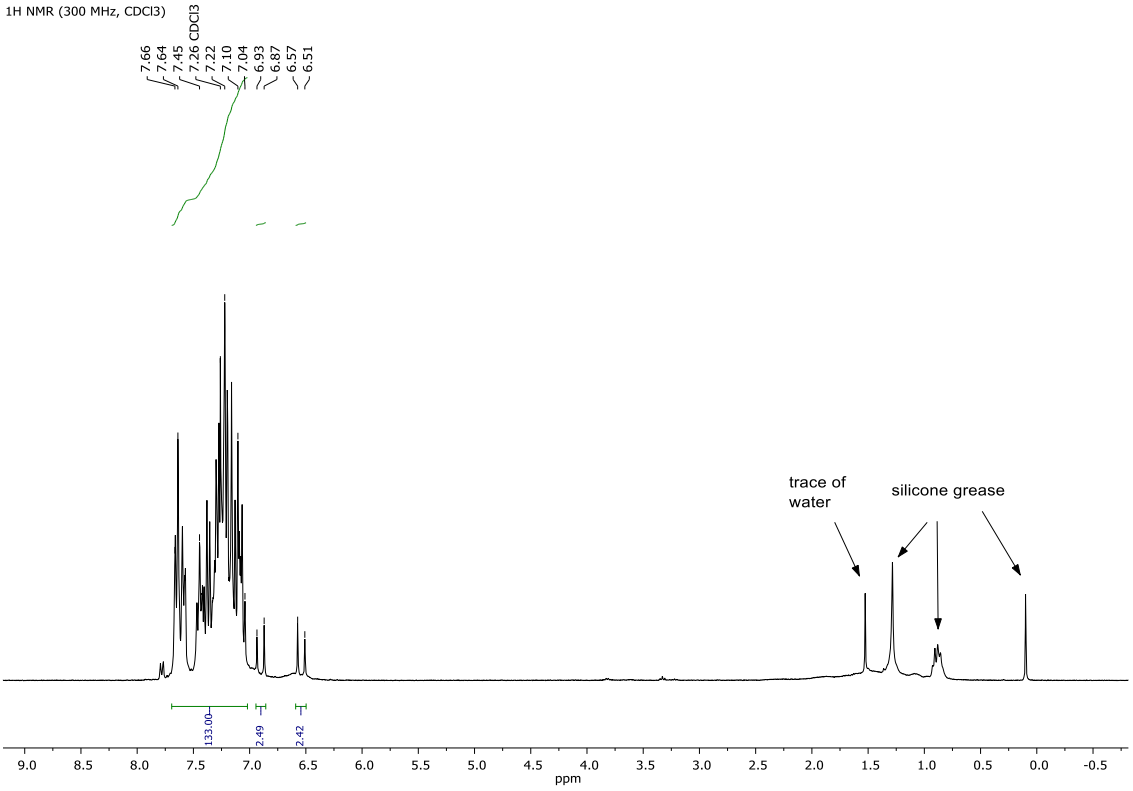

Figure S 29 ^{1}H NMR spectrum of mixture after SC of SQ-Td1c in $CDCl_3$, 300 MHz.

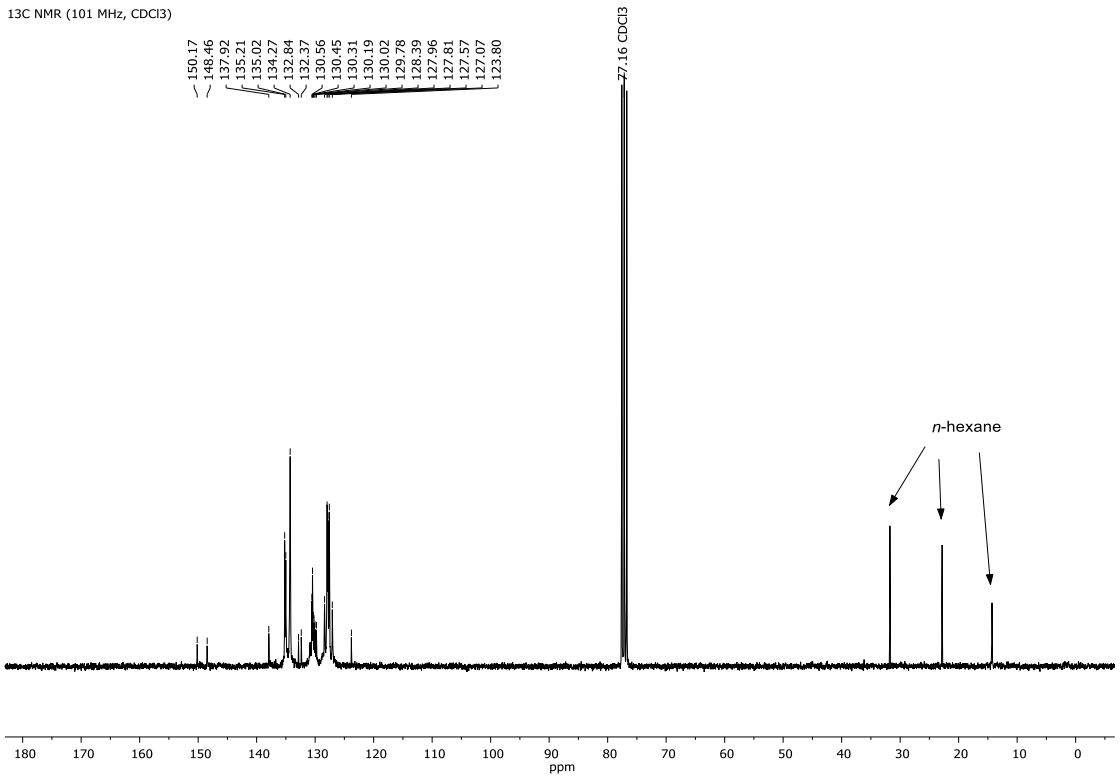

Figure S 30 ^{13}C NMR spectrum of mixture after SC of SQ-Td1c in $CDCl_3$, 101 MHz.

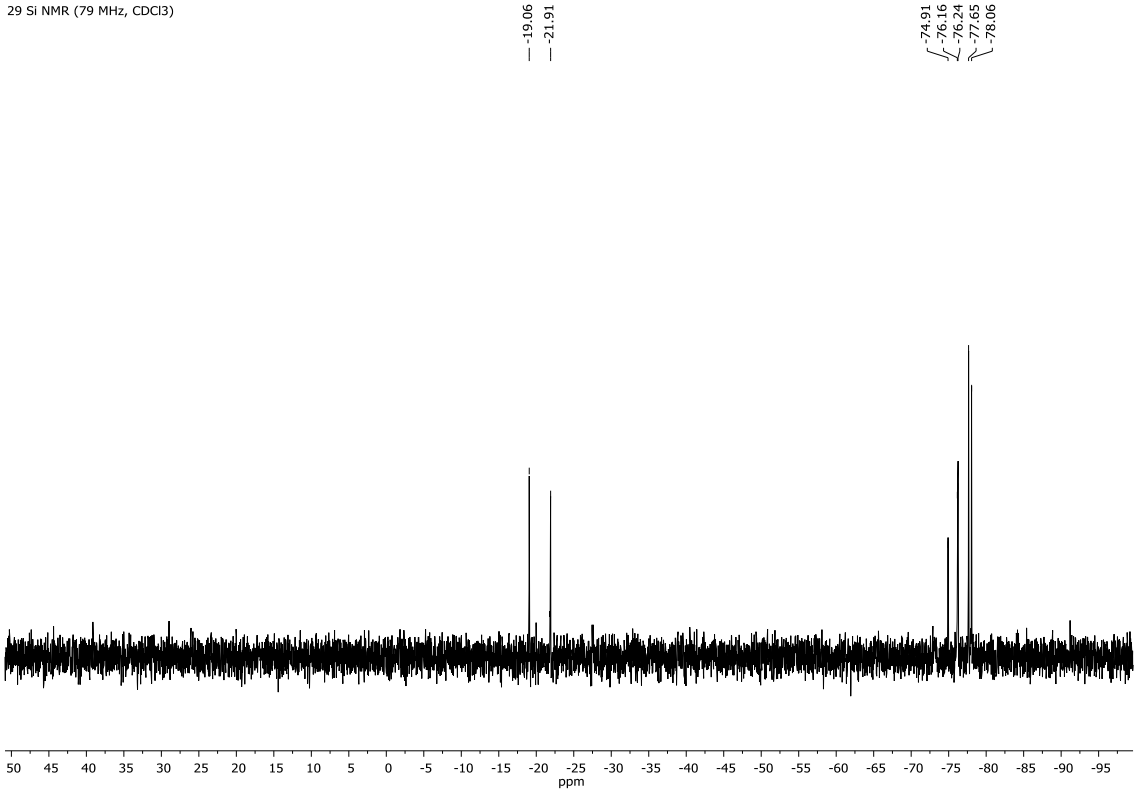

Figure S 31 ^{29}Si NMR spectrum of mixture after SC of SQ-Td1c in $CDCl_3$.

4.3 Tests for silylative homo-coupling of SQ-T1b vs. SQ-Td1c

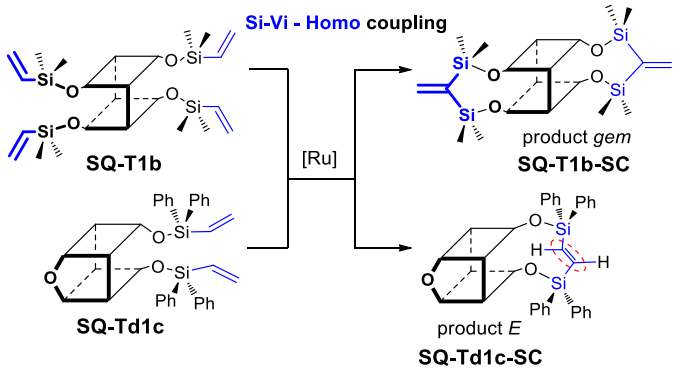

Scheme S 1. The synthetic path for silylative homo-coupling of SQ-T1b vs. SQ-Td1c

SQ-T1b-SC

White solid. Isolated Yield 89%.

^{1}H NMR (300 MHz, $CDCl_3$): δ/ppm = 7.42-7.03 (m, 40H, Ph), 6.23 (s, 4H, $=CH_2$), 0.21 (s, 24H, $-Si(CH_3)_2$).
^{13}C NMR (101 MHz, $CDCl_3$): δ/ppm = 155.35 ($-C=CH_2$), 140.38 ($-C=CH_2$), 134.27, 134.16, 133.21, 131.79, 130.16, 129.94, 127.61 (Ph), 0.94, 0.91 ($-Si(CH_3)_2$).
^{29}Si NMR (79,5 MHz, $CDCl_3$): δ/ppm = 2.63 ($-Si(CH_3)_2$), -78.52, -80.30.
IR (ATR): 3073.10, 3051.22 (C-H phenyl), 3006.66 (=C-H), 2955.95, 2924.88 (C-H), 1593.76, 1429.75 (C=C phenyl), 1256.65 (Si-C), 1129.89, 1075.72, 1029.16(Si-O-Si), 998.43 (C-H phenyl).
EA: Anal. calcd for $C_{60}H_{68}O_{14}Si_{12}$ (%):C, 53.37, H, 5.08; found: C, 53.42; H, 5.13.
ESI-MS: Calcd. for $C_{60}H_{68}Na^{+}O_{14}Si_{12}$: *m/z* 1371.1732 [M + Na^{+}]. Found: 1371.1725.

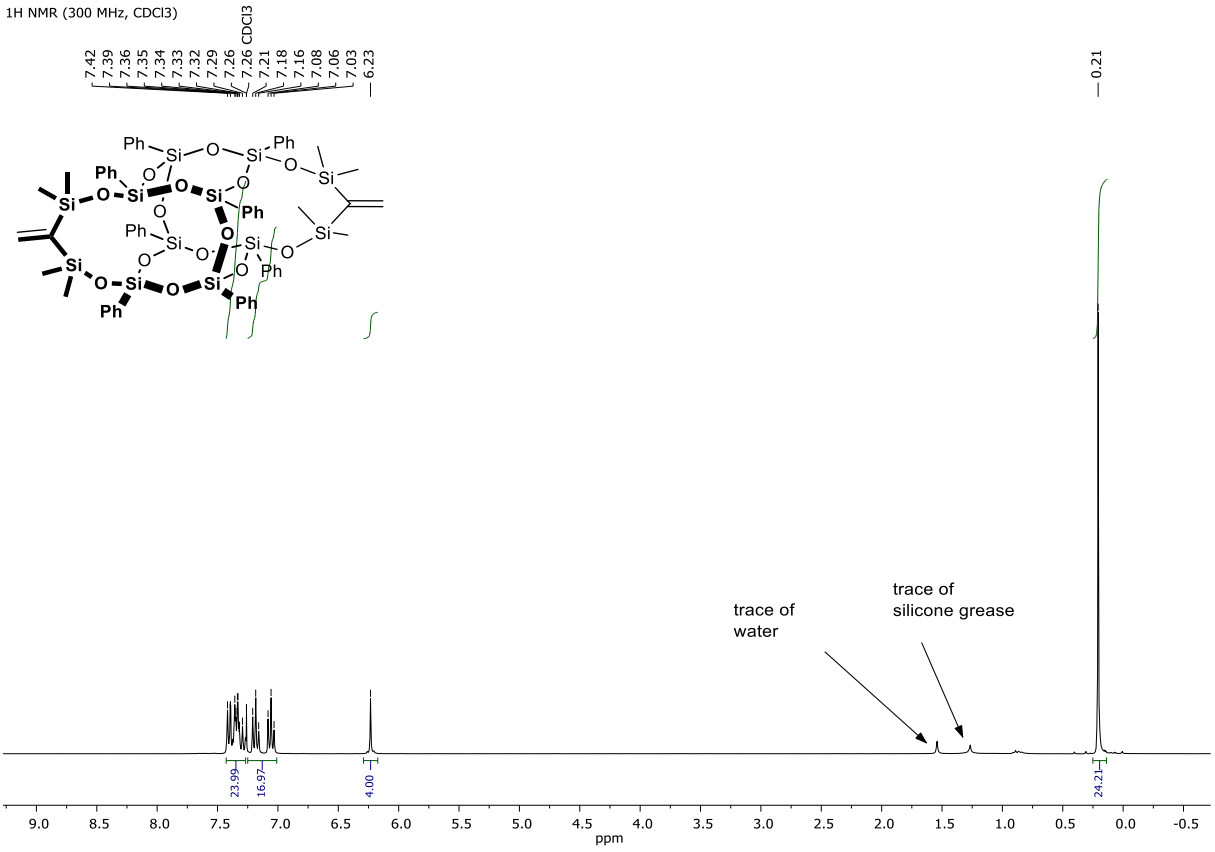

Figure S 32 ^{1}H NMR spectrum of SQ-T1b-SC in $CDCl_3$, 300 MHz.

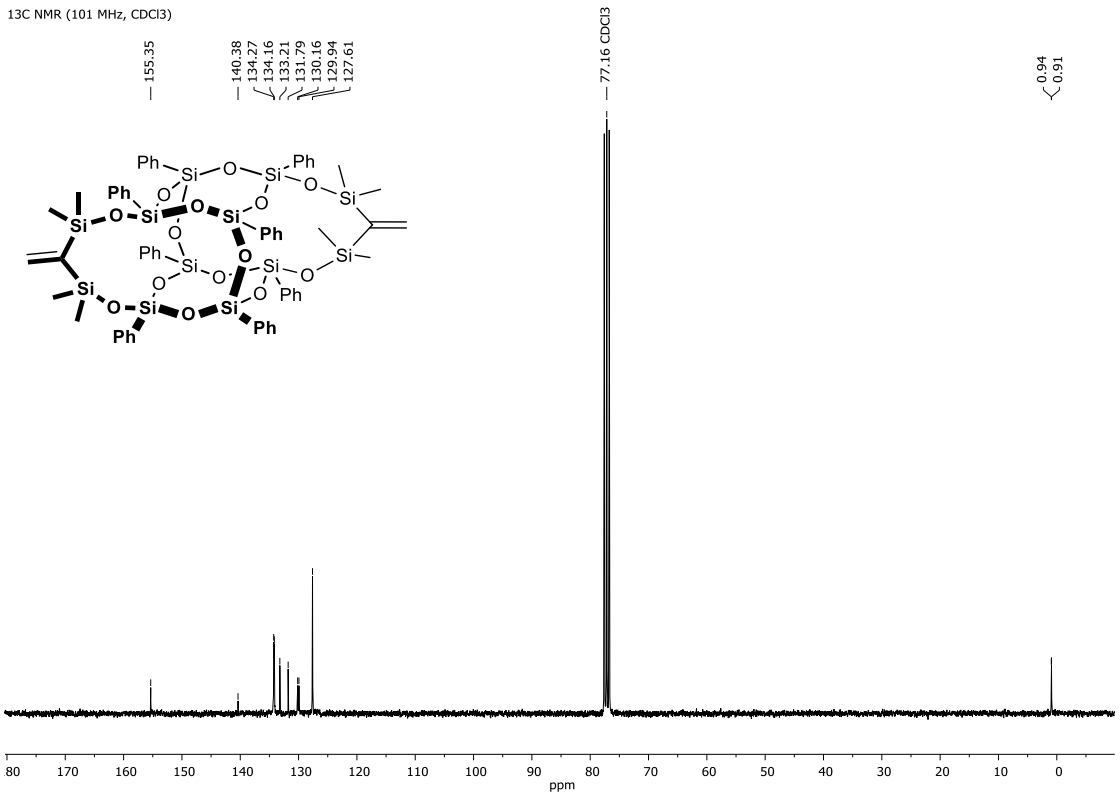

Figure S 33 ^{13}C NMR spectrum of SQ-T1b-SC in $CDCl_3$, 101 MHz.

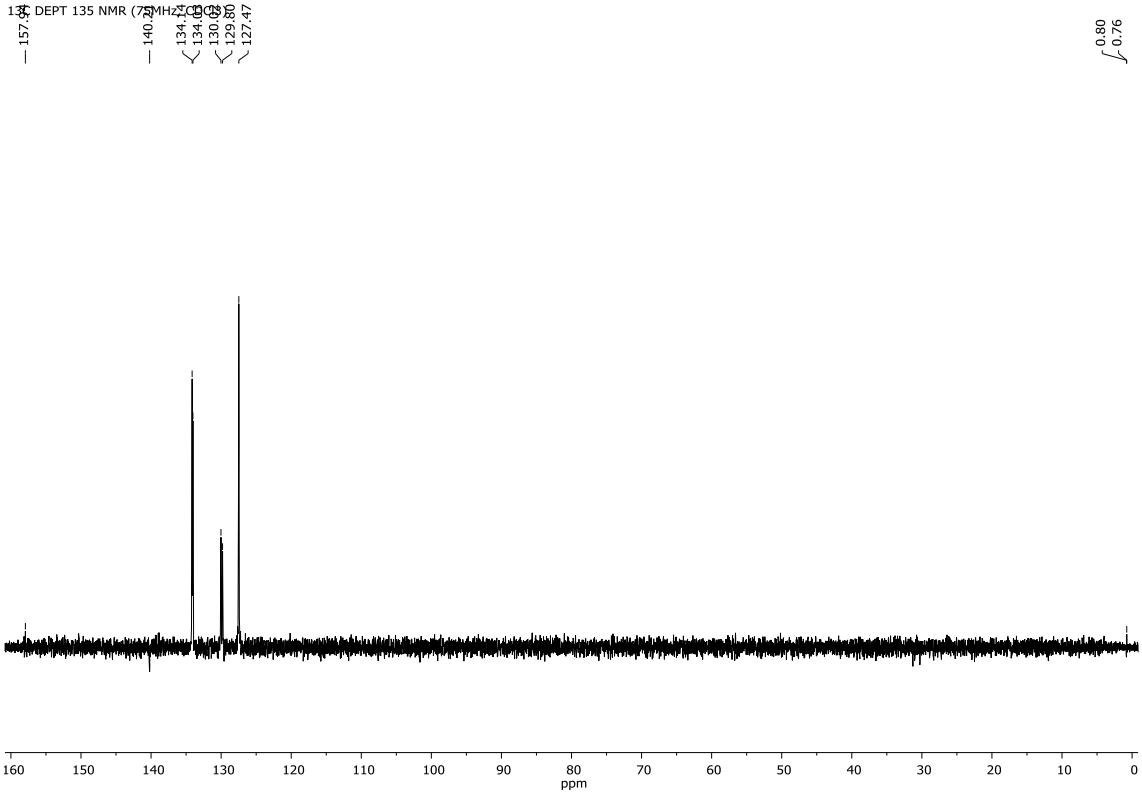

Figure S 34 ^{13}C NMR DEPT 135 spectrum of SQ-T1b-SC in $CDCl_3$, 75 MHz.

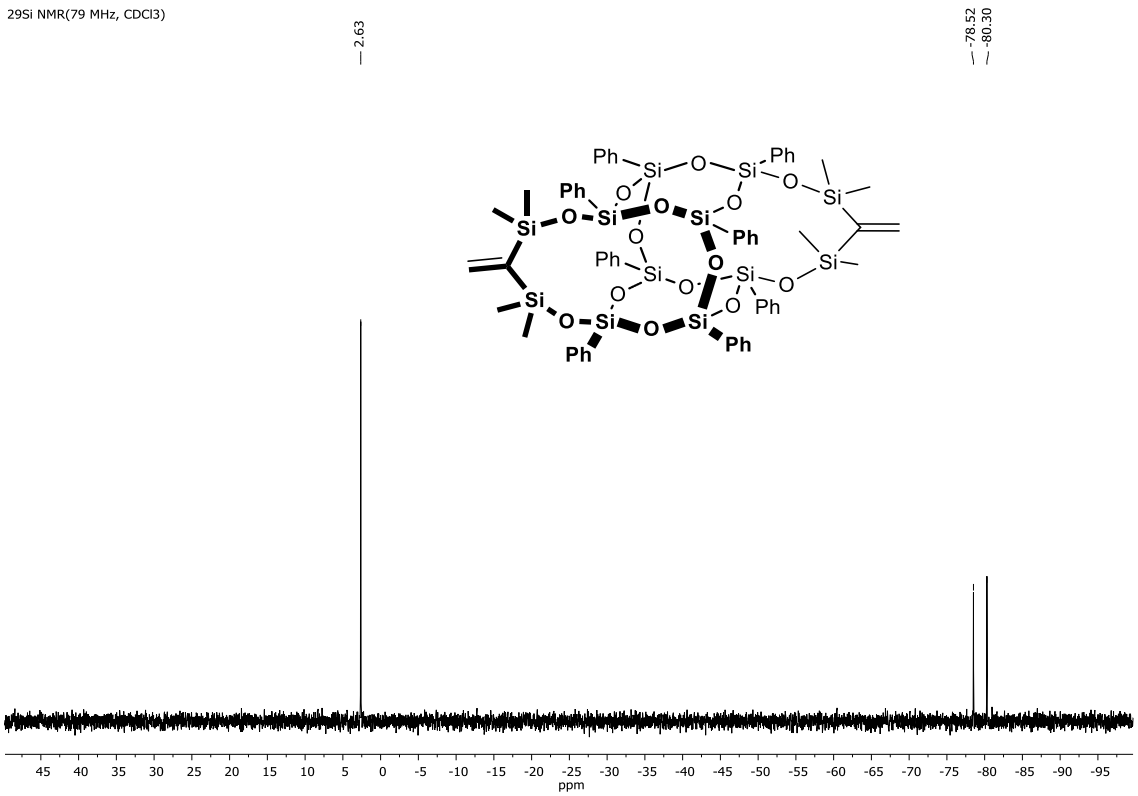

Figure S 35 ^{29}Si NMR spectrum of SQ-T1b-SC in $CDCl_3$, 79 MHz.

SQ-Td1c-SC

White solid. Isolated Yield 85%.
^{1}H NMR ($CDCl_3$, 300 MHz): δ/ppm = 7.65-7.09 (m, 62H, Ph, CH),
^{13}C NMR ($CDCl_3$, 101 MHz): δ/ppm = 150.16 (H**C**=CH), 135.20 (Ph), 135.01, 134.26, 132.36 (HC=**C**H), 130.90-130.02 (Ph), 128.01, 127.95, 127.58.
^{29}Si NMR ($CDCl_3$, 79 MHz): δ/ppm = -21.93, -76.17, -76.27, -78.93.
IR (ATR): 3070.70, 3049.14 (C-H phenyl), 3024.76 (=C-H), 1593.70, 1428.84 (C=C phenyl), 1263.54 (Si-C), 1062.49, 1027.24 (Si-O-Si), 997.46 (C-H phenyl).
EA: Anal. calcd for $C_{74}H_{62}O_{13}Si_{10}$ (%):C, 61.72, H, 4.34; found: C, 61.96; H, 4.65.
ESI-MS: Calcd. for $C_{74}H_{62}Na^{+}O_{13}Si_{10}$: *m/z* 1461.1775 [M + Na^{+}]. Found: 1461.1763.

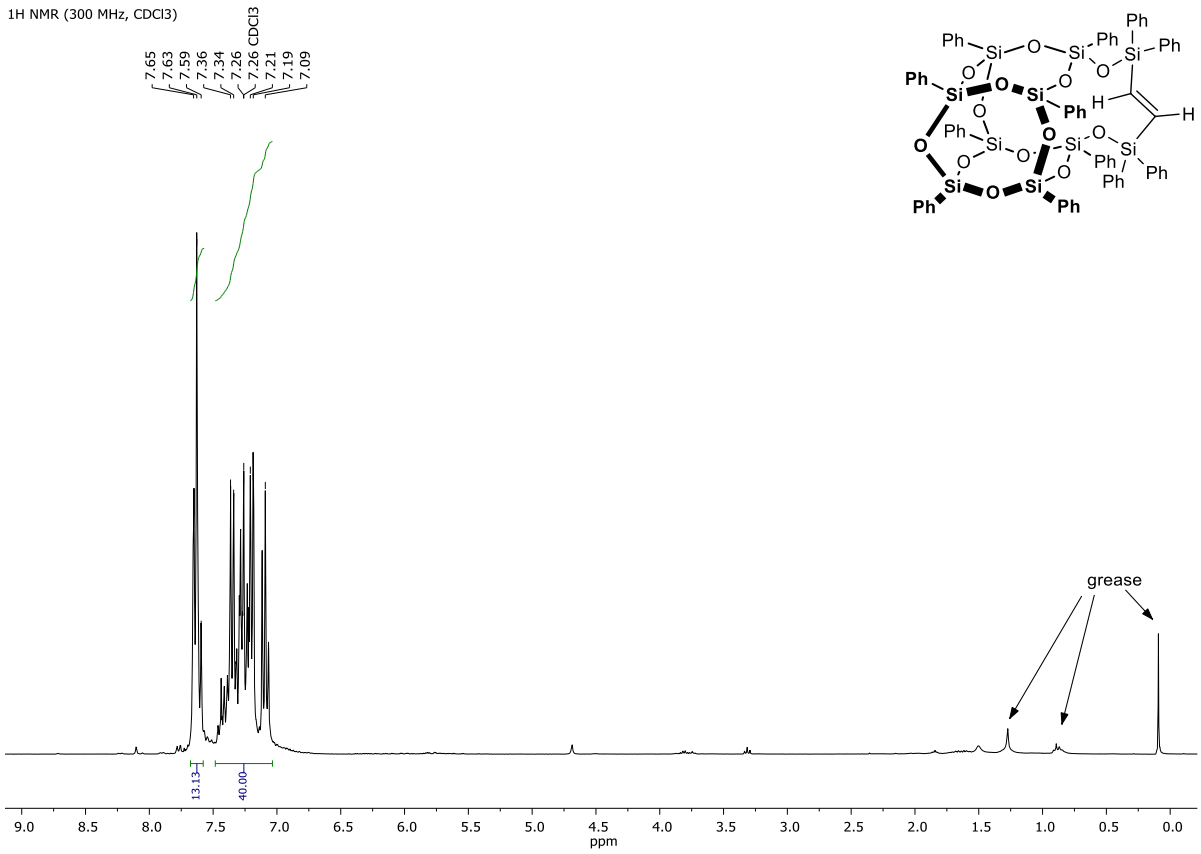

Figure S 36 ^{1}H NMR spectrum of SQ-Td1c-SC in $CDCl_3$, 300 MHz.

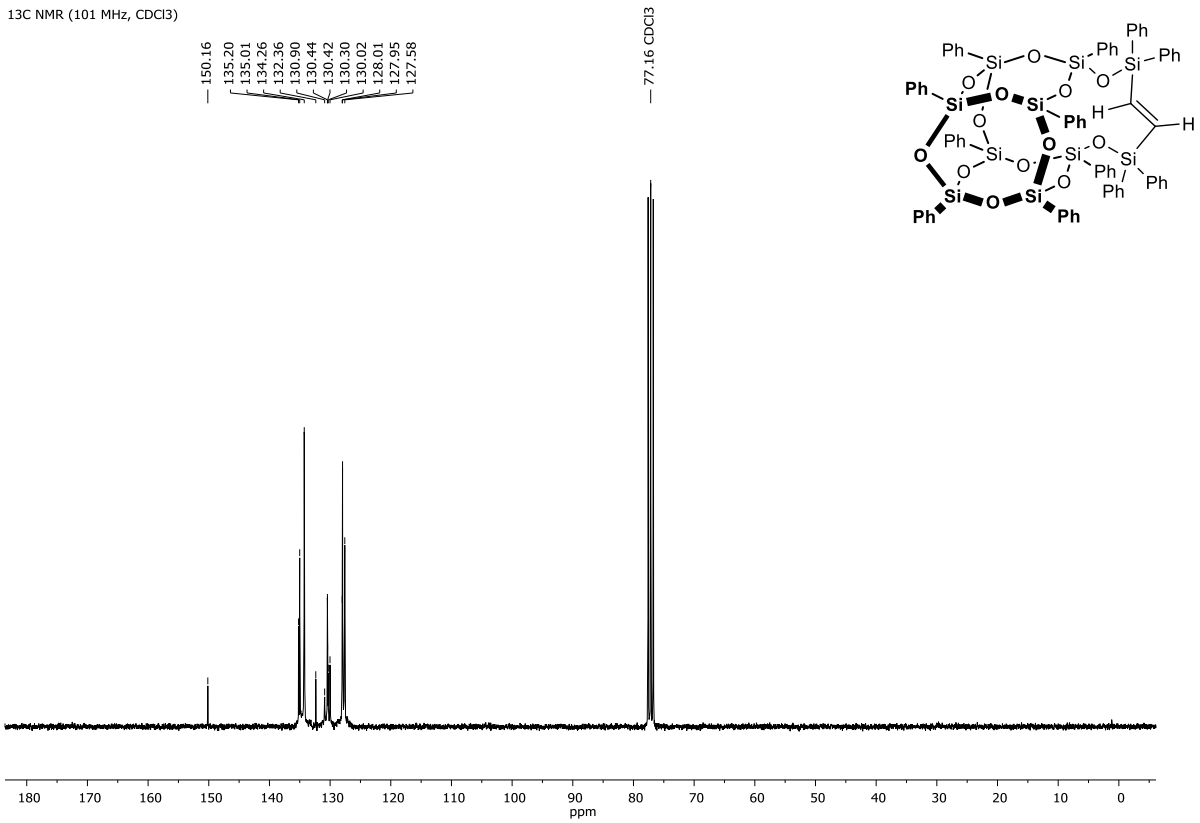

Figure S 37 ^{13}C NMR spectrum of SQ-Td1c in $CDCl_3$, 101 MHz.

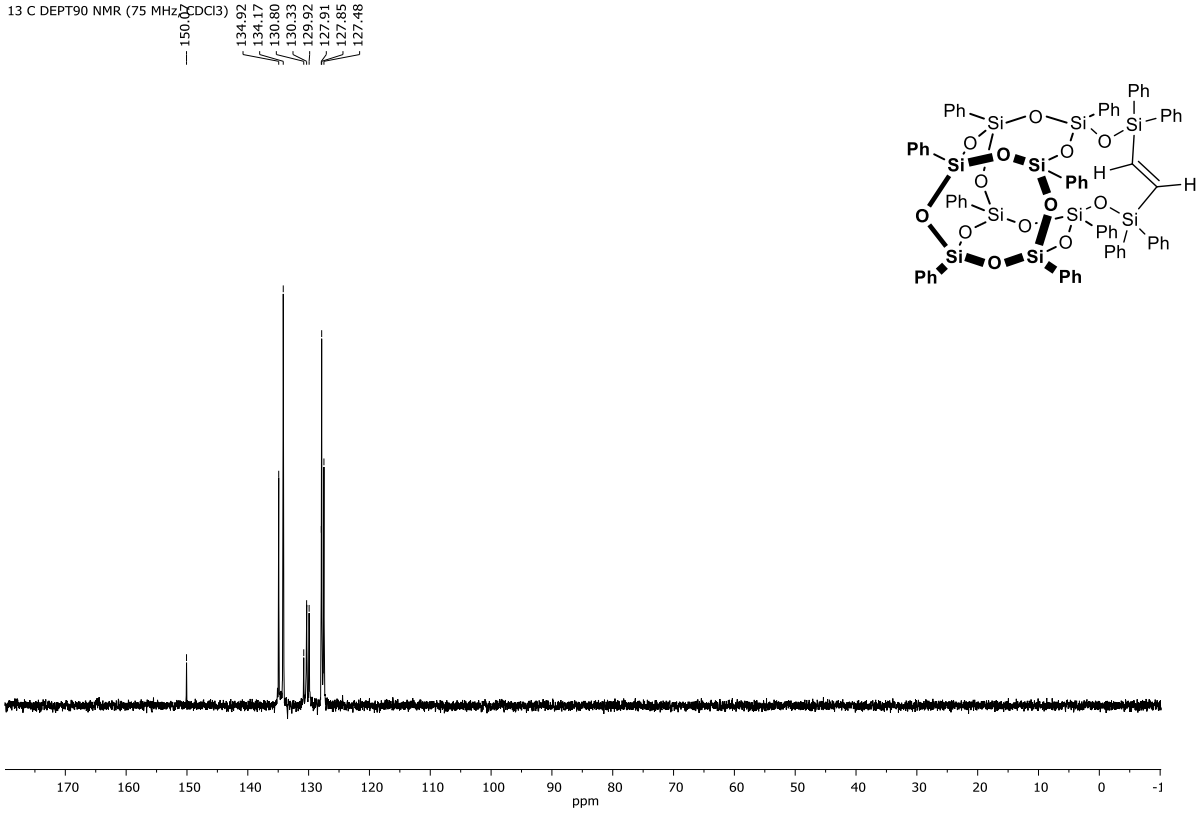

Figure S 42 ^{13}C NMR DEPT 90 spectrum of SQ-Td1c-SC in $CDCl_3$, 75 MHz.

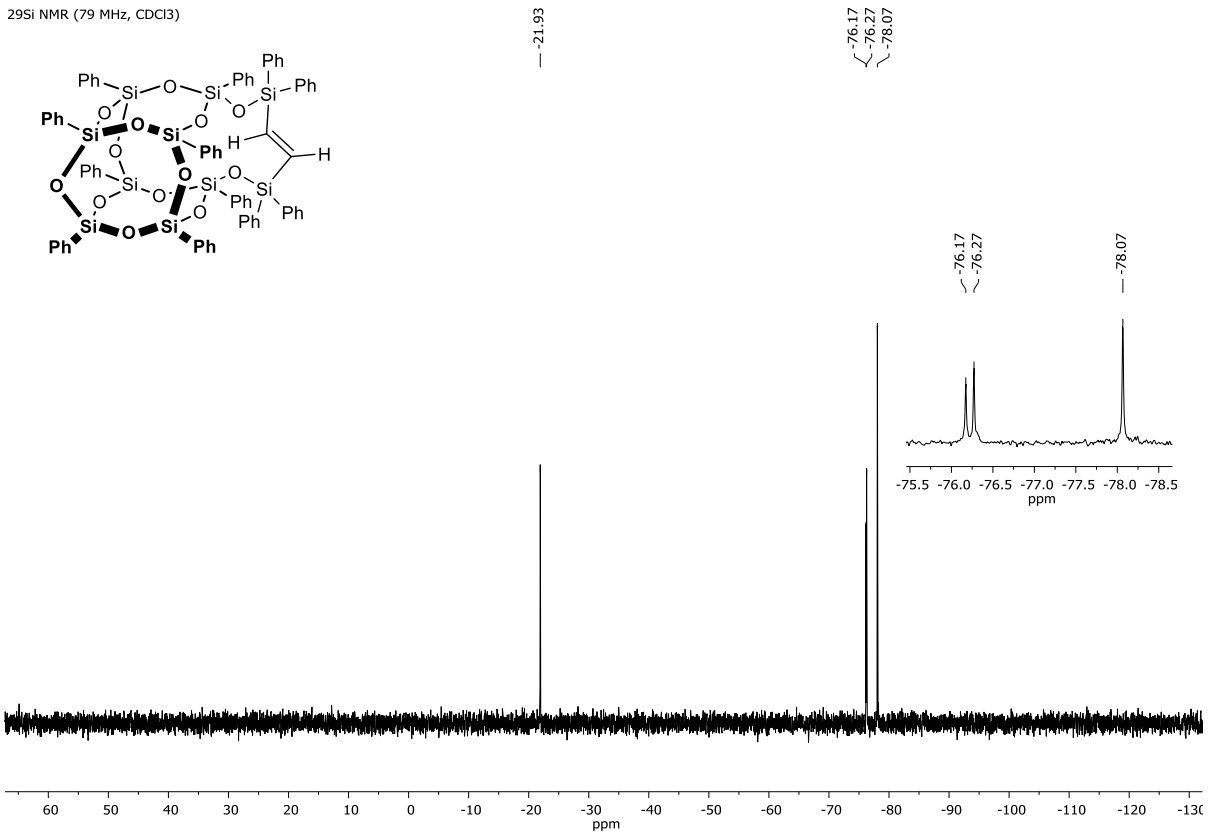

Figure S 38 ^{29}Si NMR spectrum of SQ-Td1c-SC in $CDCl_3$, 79 MHz.

5. Spectrometric analysis

5.1. MALDI-TOF MS analysis

Table S 2 Observed MALDI-TOF peaks found for sodium adducts [M+Na]+for HC reaction of SQ-4OH with 1a.

Compound formula	Calcd. m/z	Measur. m/z	Error [ppm]
Sample a			
$C_{58}H_{64}Cl_2O_{13}Si_{10}Na^+$	1341.1309	1341.1297	0.9
$C_{58}H_{66}Cl_2O_{14}Si_{10}Na^+$	1359.1414	1359.1413	0.1
$C_{63}H_{77}Cl_3O_{14}Si_{11}Na^+$	1493.1733	1493.1757	1.6
Sample b			
$C_{58}H_{64}Cl_2O_{13}Si_{10}Na^+$	1341.1309	1341.1231	5.8
$C_{58}H_{66}Cl_2O_{14}Si_{10}Na^+$	1359.1414	1359.1320	6.9
$C_{63}H_{77}Cl_3O_{14}Si_{11}Na^+$	1493.1733	1493.1713	1.3
$C_{68}H_{88}Cl_4O_{14}Si_{12}Na^+$	1627.2052	1627.1994	3.7
Sample c			
$C_{58}H_{64}Cl_2O_{13}Si_{10}Na^+$	1341.1309	1341.1266	3.2
$C_{58}H_{66}Cl_2O_{14}Si_{10}Na^+$	1359.1414	1359.1298	8.5
$C_{63}H_{77}Cl_3O_{14}Si_{11}Na^+$	1493.1733	1493.1686	3.1
$C_{68}H_{88}Cl_4O_{14}Si_{12}Na^+$	1627.2052	1627.2065	0.8
Sample d			
$C_{58}H_{64}Cl_2O_{13}Si_{10}Na^+$	1341.1309	1341.1317	0.6
$C_{63}H_{77}Cl_3O_{14}Si_{11}Na^+$	1493.1733	1493.1766	2.2
$C_{68}H_{88}Cl_4O_{14}Si_{12}Na^+$	1627.2052	1627.2065	0.8
Sample e			
$C_{58}H_{64}Cl_2O_{13}Si_{10}Na^+$	1341.1309	1341.1387	6
$C_{68}H_{88}Cl_4O_{14}Si_{12}Na^+$	1627.2052	1627.2049	0.2

5.2. ESI-MS analysis

The procedure for the preparation of ESI- MS specimens was performed in analogous methodology as MALDI-TOF MS and the description of respective samples is below:

f) - after 15 minutes from the start of the silane (1a) dropwise addition,
g) - just after complete addition of 1a,
h) - 1 h after complete addition of 1a,
i) - 2 h after complete addition of 1a,
j) - 12 h after complete addition of 1a,
k) - 24 h after complete addition of 1a.

All of the specimens were taken from the reaction mixture, filtrated (of triethylammonium chloride salt) and evaporated under reduced pressure. They were then dissolved in DCM/methanol solution and measured by ESI-MS. For this analysis, the sodium adducts were mainly observed, but for the incompletely condensed product with three 3-chloropropyl groups, the adducts with Na^+ and Et_3NH^+ were also present. Despite the filtration of the reaction mixture, the ESI-MS analysis showed the presence of traces of amine residue.

Signals derived from Ph8T8 by-product visible 1H NMR spectra of the post-reaction mixture are again omitted on MS spectra's for clearance (Ph_8T_8 [M+Na]+ 1055.3).

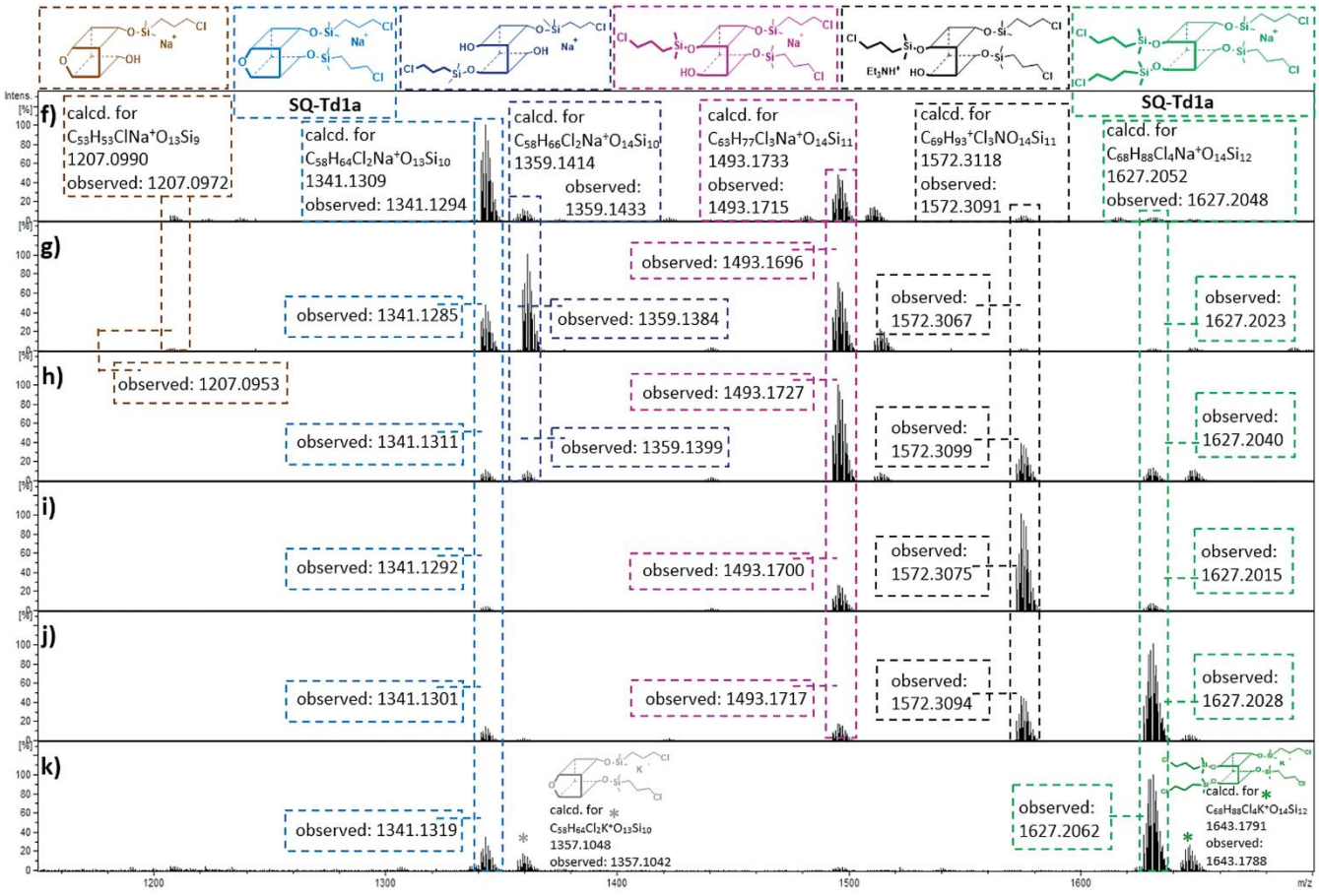

Figure S 39 Stacked ESI-MS spectra for HC reaction of **SQ-4OH** with **1a** within time (a – e).

Table S 3 Observed ESI-MS peaks found for sodium/amine adducts $[M+Na/Et_3NH]^+$ for HC reaction of SQ-4OH with 1a

Compound formula	Calcd. m/z	Measur. m/z	Error [ppm]
Sample f			
$C_{53}H_{53}ClO_{13}Si_9Na^+$	1207.0990	1207.0927	1.5
$C_{58}H_{64}Cl_2O_{13}Si_{10}Na^+$	1341.1309	1341.1294	1.2
$C_{58}H_{66}Cl_2O_{14}Si_{10}Na^+$	1359.1415	1359.1433	1.3
$C_{63}H_{77}Cl_3O_{14}Si_{11}Na^+$	1493.1733	1493.1715	1.2
$C_{69}H_{93}{}^+Cl_3NO_{14}Si_{11}$	1572.3118	1572.3091	1.8
$C_{68}H_{88}Cl_4O_{14}Si_{12}Na^+$	1627.2052	1627.2048	0.2
Sample g			
$C_{53}H_{53}ClO_{13}Si_9Na^+$	1207.0990	1207.0953	3.1
$C_{58}H_{64}Cl_2O_{13}Si_{10}Na^+$	1341.1309	1341.1285	1.8
$C_{58}H_{66}Cl_2O_{14}Si_{10}Na^+$	1359.1414	1359.1384	2.3
$C_{63}H_{77}Cl_3O_{14}Si_{11}Na^+$	1493.1733	1493.1696	2.5
$C_{69}H_{93}{}^+Cl_3NO_{14}Si_{11}$	1572.3118	1572.3067	3.2
$C_{68}H_{88}Cl_4O_{14}Si_{12}Na^+$	1627.2052	1627.2023	1.8
Sample h			
$C_{58}H_{64}Cl_2O_{13}Si_{10}Na^+$	1341.1309	1341.1311	0.1
$C_{58}H_{66}Cl_2O_{14}Si_{10}Na^+$	1359.1414	1359.1399	1.2
$C_{63}H_{77}Cl_3O_{14}Si_{11}Na^+$	1493.1733	1493.1727	0.4
$C_{69}H_{93}{}^+Cl_3NO_{14}Si_{11}$	1572.3118	1572.3099	1.2
$C_{68}H_{88}Cl_4O_{14}Si_{12}Na^+$	1627.2052	1627.2040	0.7
Sample i			
$C_{58}H_{64}Cl_2O_{13}Si_{10}Na^+$	1341.1309	1341.1292	1.3
$C_{63}H_{77}Cl_3O_{14}Si_{11}Na^+$	1493.1733	1493.1700	2.2
$C_{69}H_{93}{}^+Cl_3NO_{14}Si_{11}$	1572.3118	1572.3075	2.7
$C_{68}H_{88}Cl_4O_{14}Si_{12}Na^+$	1627.2052	1627.2015	2.3
Sample j			
$C_{58}H_{64}Cl_2O_{13}Si_{10}Na^+$	1341.1309	1341.1301	0.6
$C_{63}H_{77}Cl_3O_{14}Si_{11}Na^+$	1493.1733	1493.1717	1.1
$C_{69}H_{93}{}^+Cl_3NO_{14}Si_{11}$	1572.3118	1572.3094	1.5
$C_{68}H_{88}Cl_4O_{14}Si_{12}Na^+$	1627.2052	1627.2028	1.4
Sample k			
$C_{58}H_{64}Cl_2O_{13}Si_{10}Na^+$	1341.1309	1341.1301	0.7
$C_{68}H_{88}Cl_4O_{14}Si_{12}Na^+$	1627.2052	1627.2028	0.6

6. TGA/DSC analysis

Table S 4 Thermal properties of obtained compounds measured in N_2.

Prod. Abbreviation	Mass loss Temperature [°C]		Residue at 1000 °C [%]
	$T_d^{5\%}$	$T_d^{10\%}$	
SQ-T1a	292	314	11
SQ-Td1a	291	371	13
SQ-D2a	306	370	43
SQ-Dm2a	369	405	35
SQ-T1b	381	416	37
SQ-Td1b	397	437	44
SQ-D2b	391	530	78
SQ-Dm2b	495	551	79
SQ-T1c	423	456	31
SQ-Td1c	431	464	39
SQ-T1d	373	413	27
SQ-Td1d	379	403	32
SQ-D2d	393	429	57
SQ-Dm2d	397	428	48
SQ-T1b-SC	386	415	48
SQ-Td1c-SC	451	473	36

Table S 5 Melting points of obtained compounds - assigned by DSC method

Prod. Abbreviation	Melting point
SQ-T1a	98.67 ℃
SQ-Td1a	133.00 ℃
SQ-D2a	272.00 ℃
SQ-Dm2a	233.00 ℃
SQ-T1b	146.67 ℃
SQ-Td1b	233.50 ℃
SQ-D2b	214.83 ℃
SQ-Dm2b	238.17 ℃
SQ-Td1c	169.00 ℃
SQ-T1d	109.50 ℃
SQ-Td1d	145.67 ℃
SQ-D2d	220.00 ℃
SQ-Dm2d	211.83 ℃
SQ-T1b-SC	233.17 ℃
SQ-Td1c-SC	291.44 ℃

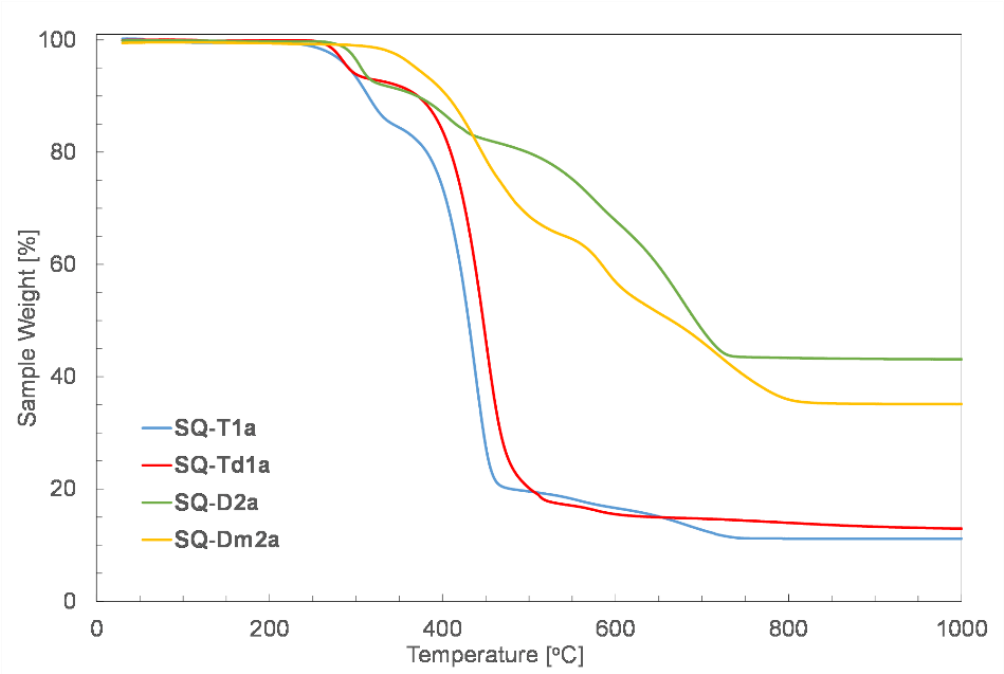

Figure S 40 TGA analysis of open- and closed-cage SQs with 3-chloropropyl group(s) performed in N_2.

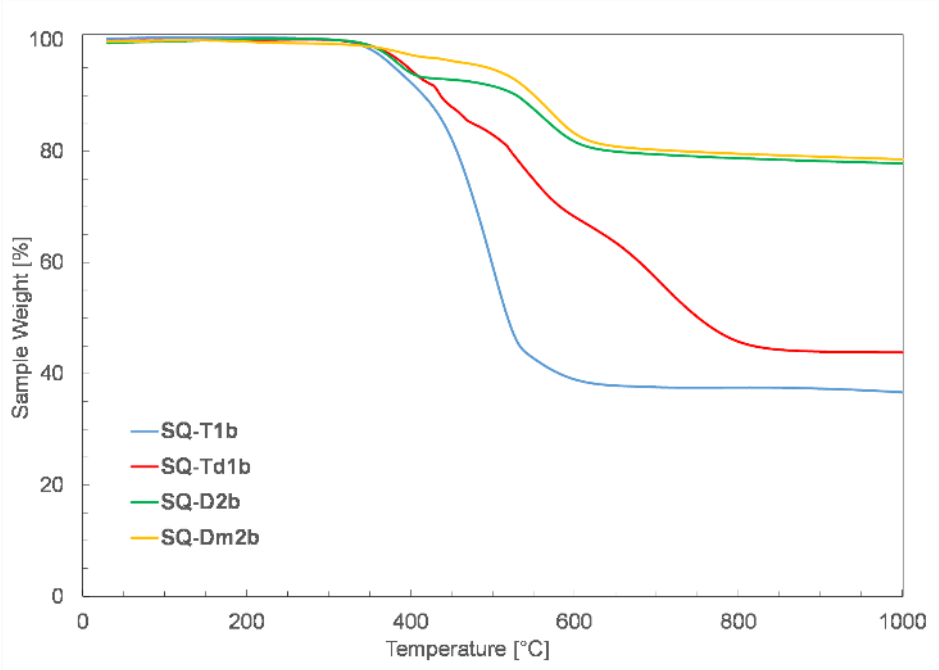

Figure S 41 TGA analysis of open- and closed-cage SQs with vinyl group(s) performed in N_2.

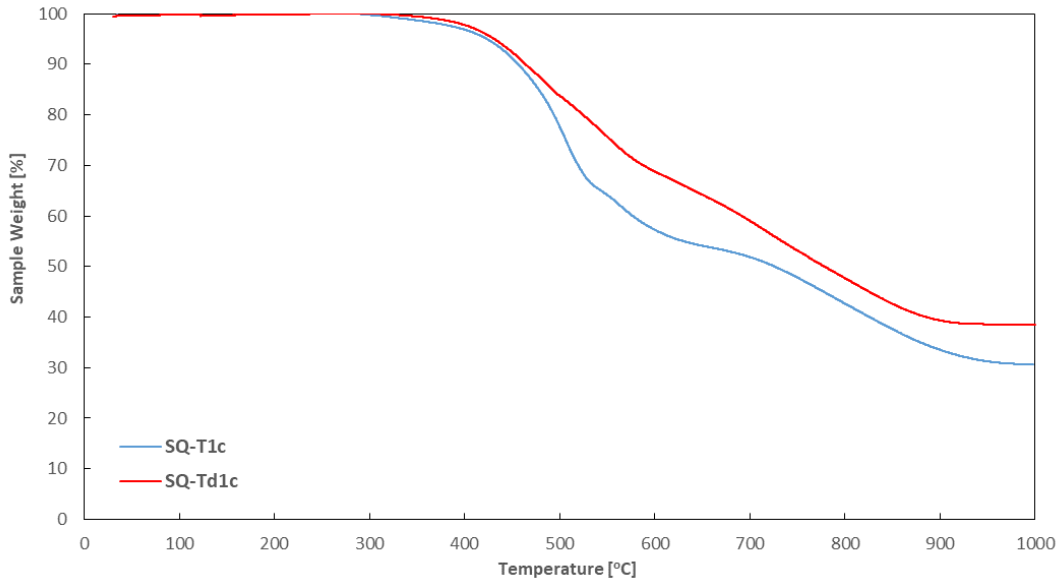

Figure S 42 TGA analysis of HC products performed in a nitrogen.

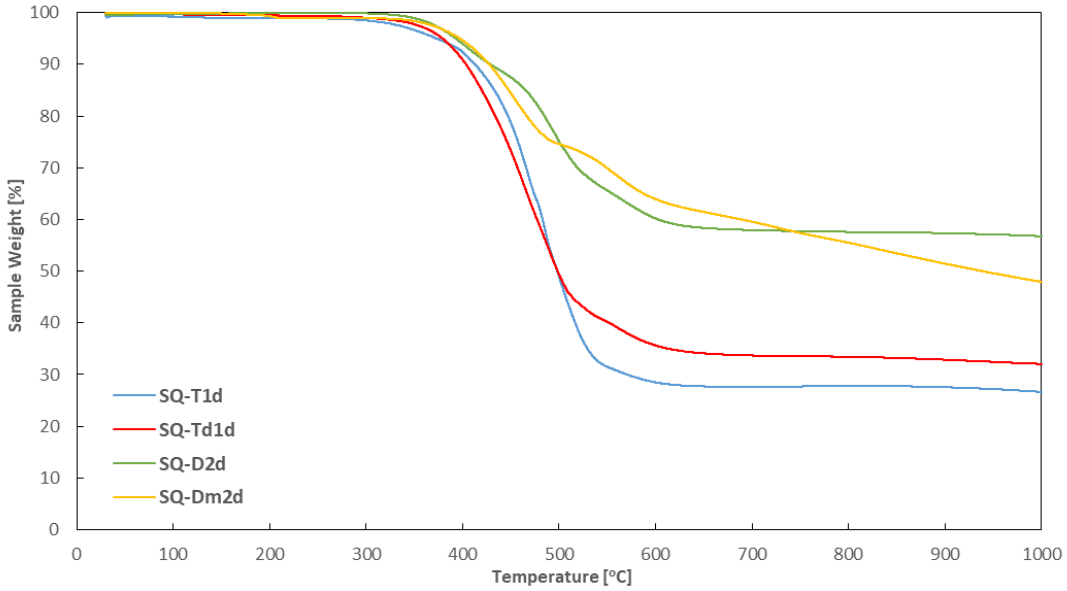

Figure S 43 TGA analysis of HC products performed in a nitrogen.

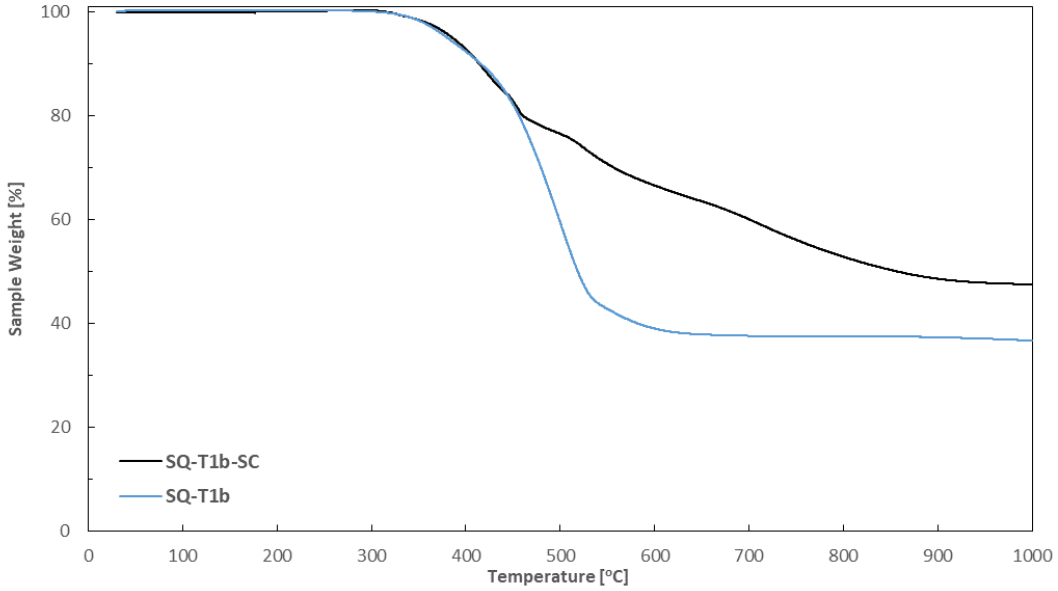

Figure S 44 TGA analysis of SC products performed in a nitrogen.

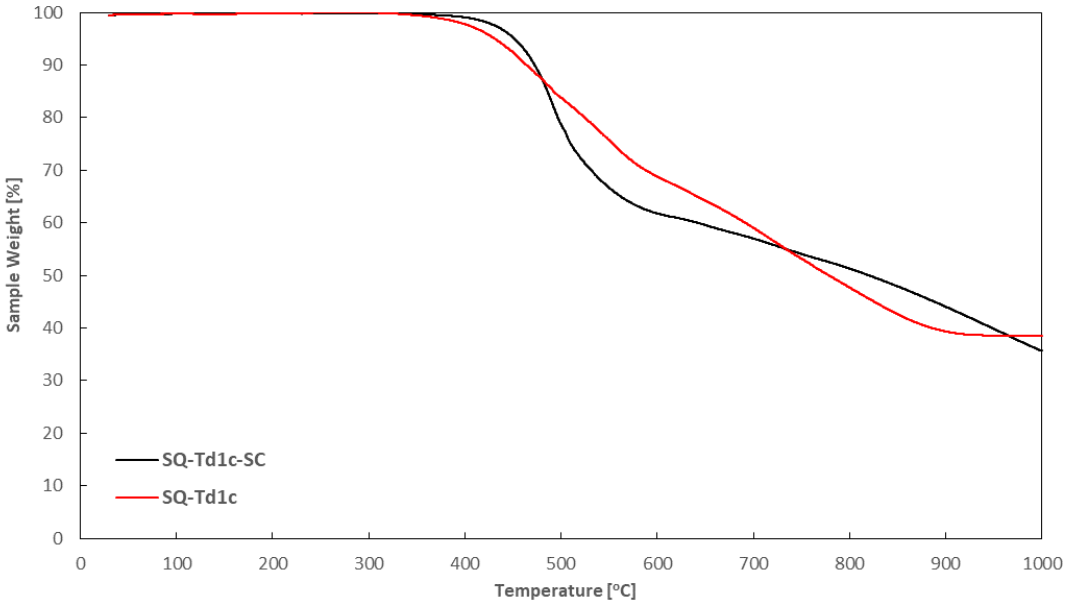

Figure S 45 TGA analysis of SC products performed in a nitrogen.

7. X-ray Analysis

Table S 6 Crystal data, data collection and structure refinement

Compound	**SQ-T1a**	**SQ-Td1a**	**SQ-Td1b**	**SQ-Td1c**
Formula	$C_{68}H_{88}Cl_4O_{14}Si_{12}$	$C_{58}H_{64}Cl_2O_{13}Si_{10}$	$C_{56}H_{58}O_{13}Si_{10}$	$C_{76}H_{66}O_{13}Si_{10}$
Formula weight	1608.26	1320.89	1219.92	1468.18
Crystal system	triclinic	triclinic	Monoclinic	triclinic
Space group	P-1	P-1	Pn	P-1
a(Å)	12.8421(5)	11.2359(4)	10.98072(18)	13.7102(3)
b(Å)	16.9319(6)	14.4348(4)	10.69865(19)	14.9905(3)
c(Å)	18.6056(7)	20.6432(6)	26.0350(4)	20.0608(4)
α(°)	90.263(3)	104.503(3)	90	97.619(2)
β(º)	91.075(3)	91.243(2)	101.2833(16)	92.684(2)
γ(°)	93.084(3)	100.119(3)	90	115.487(2)
V(Å^3)	4039.0(3)	3183.38(18)	2999.45(9)	3663.91(14)
Z	2	2	2	2
D_x(g cm^{-3})	1.322	1.378	1.351	1.331
F(000)	1688	1380	1276	1532
μ(mm^{-1})	0.382	0.351	0.280	0.242
Reflections:				
collected	43342	23840	19596	32769
unique (R_{int})	18920 (0.0404)	12340 (0.0227)	9591 (0.0172)	15021 (0.0186)
with I>2σ(I)	16184	10651	9264	14262
R(F) [I>2σ(I)]	0.0360	0.0344	0.0272	0.0660
wR(F^2) [I>2σ(I)]	0.0899	0.0839	0.0702	0.1888
R(F) [all data]	0.0458	0.0418	0.0288	0.0681
wR(F^2) [all data]	0.0924	0.0885	0.0715	0.1912
Goodness of fit	1.028	1.024	1.033	0.997
max/min Δ (e·Å^{-3})	0.49/-0.36	0.66/-0.61	0.91/-0.23	0.77/-0.69
CCDC number	2041825	2041826	2058969	2051014

Compound	**SQ-T1d**	**SQ-Td1d**	**SQ-Dm2a**	**SQ-Dm2b**
Formula	$C_{68}H_{84}O_{14}Si_{12}$	$C_{58}H_{62}O_{13}Si_{10}$	$C_{52}H_{49}ClO_{13}Si_9$	$C_{51}H_{46}O_{13}Si_9$
Formula weight	1462.43	1247.97	1608.1170.17	1119.69
Crystal system	monoclinic	triclinic	monoclinic	monoclinic
Space group	P2/n	P-1	$P2_1/c$	$P2_1/c$
a(Å)	12.8971(3)	11.0889(5)	14.0582(5)	17.6363(2)
b(Å)	18.3850(4)	14.6164(5)	16.8552(7)	10.91209(17)
c(Å)	16.7859(4)	20.2859(8)	23.5988(9)	27.9552(4)
α(°)	90	75.800(3)	90	90
β(º)	91.586(2)	85.746(3)	98.552(3)	93.9393(13)
γ(°)	90	75.825(4)	90	90
V(Å^3)	3978.63(16)	3090.1(2)	5529.6(4)	5367.24(13)
Z	2	2	4	4
D_x(g cm^{-3})	1.221	1.341	1.406	1.386
F(000)	1544	1308	2432	2328
μ(mm^{-1})	2.316	0.274	0.327	0.285
Reflections:				
collected	19489	23022	19474	22158
unique (R_{int})	8155 (0.0405)	11955 (0.0160)	9712 (0.0370)	10388 (0.0198)

with I>2σ(I)	7386	10538	6938	8437
R(F) [I>2σ(I)]	0.0936	0.0310	0.0673	0.0419
wR(F^2) [I>2σ(I)]	0.2428	0.0772	0.1767	0.0965
R(F) [all data]	0.0997	0.0374	0.0954	0.0565
wR(F^2) [all data]	0.2452	0.0810	0.1925	0.1031
Goodness of fit	0.994	1.048	1.004	1.045
max/min Δ ($e \cdot Å^{-3}$)	1.23/-0.68	0.40/-0.28	0.50/-1.13	0.44/-0.38
CCDC number	2041827	2041828	2041829	2041830

Compound	**SQ-Dm2d**	**SQ-T1b-SC**	**SQ-Td1c-SC**
Formula	$C_{52}H_{48}O_{13}Si_9$	$C_{60}H_{68}O_{14}Si_{12}$	$C_{74}H_{62}O_{13}Si_{10}$
Formula weight	1133.71	1350.22	1440.13
Crystal system	Monoclinic	triclinic	monoclinic
Space group	$P2_1/c$	P-1	$P2_1/c$
a(Å)	14.2559(4)	13.1911(6)	10.9318(3)
b(Å)	16.7794(5)	13.5671(5)	20.1891(7)
c(Å)	23.8083(6)	13.6405(6)	33.9032(10)
α(°)	90	61.188(4)	90
β(º)	98.576(2)	68.229(4)	91.496(3)
γ(°)	90	77.731(3)	90
V($Å^3$)	5631.4(3)	1984.70(17)	7480.0(4)
Z	4	1	4
D_x(g cm^{-3})	1.337	1.130	1.279
F(000)	2360	708	3000
μ(mm^{-1})	0.273	0.247	0.236
Reflections:			
collected	25474	15301	31815
unique (R_{int})	9885 (0.0193)	7733 (0.0145)	13121 (0.0296)
with I>2σ(I)	7522	6733	7494
R(F) [I>2σ(I)]	0.0534	0.0302	0.0648
wR(F^2) [I>2σ(I)]	0.1511	0.0784	0.1705
R(F) [all data]	0.0759	0.0360	0.1136
wR(F^2) [all data]	0.1638	0.0817	0.1990
Goodness of fit	1.079	1.027	0.984
max/min Δ ($e \cdot Å^{-3}$)	0.97/-0.39	0.36/-0.28	0.30/-0.31
CCDC number	2058970	2041831	2043903

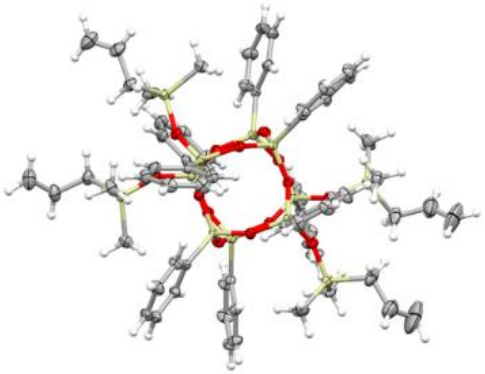

Figure S 51. A perspective view of the molecule **SQ-T1d.** Ellipsoids are drawn at the 50% probability level, hydrogen atoms are shown as spheres of arbitrary radii.

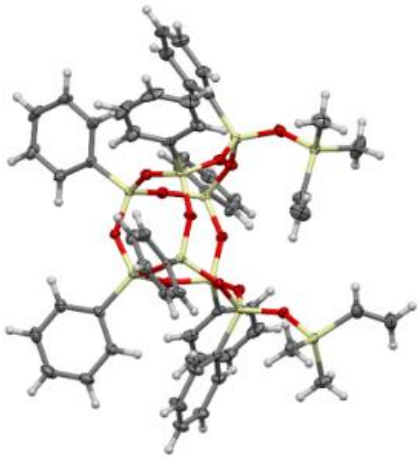

Figure S 52 A perspective view of the molecule **SQ-Td1b**. Ellipsoids are drawn at the 50% probability level, hydrogen atoms are shown as spheres of arbitrary radii.

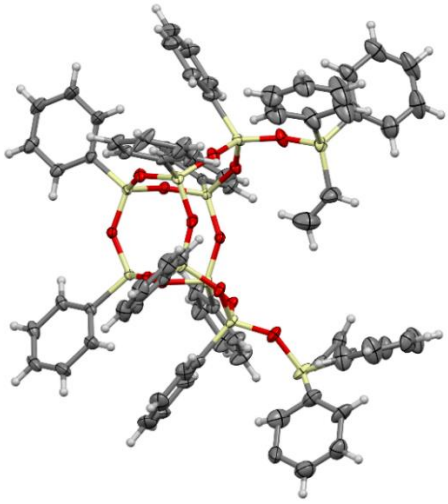

Figure S 53 A perspective view of the molecule **SQ-Td1c**. Ellipsoids are drawn at the 50% probability level, hydrogen atoms are shown as spheres of arbitrary radii.

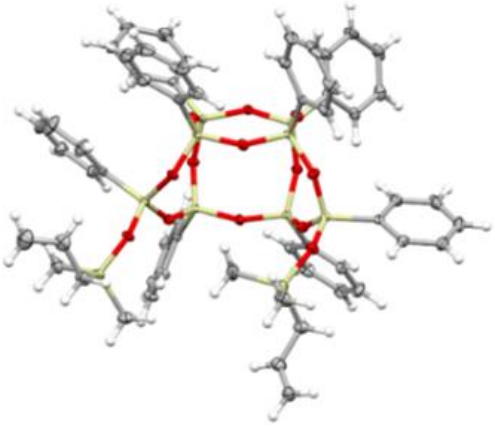

Figure S 54 A perspective view of the molecule **SQ-Td1d**. Ellipsoids are drawn at the 50% probability level, hydrogen atoms are shown as spheres of arbitrary radii.

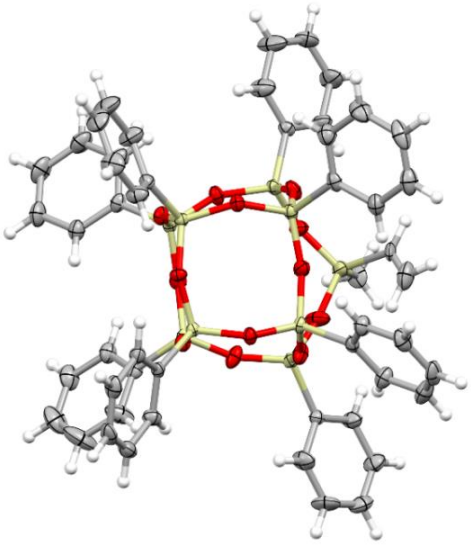

Figure S 46 A perspective view of the molecule **SQ-Dm2b**. Ellipsoids are drawn at the 50% probability level, hydrogen atoms are shown as spheres of arbitrary radii.

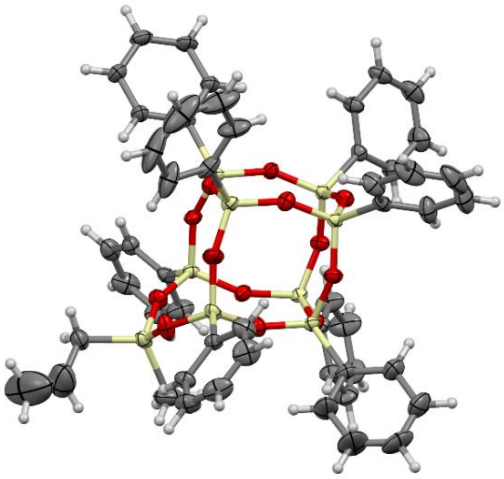

Figure S 47 A perspective view of the molecule **SQ-Dm2d**. Ellipsoids are drawn at the 50% probability level, hydrogen atoms are shown as spheres of arbitrary radii.

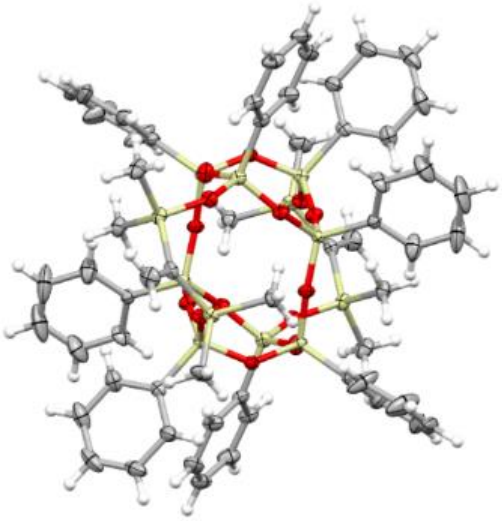

Figure S 57 A perspective view of the molecule **SQ-T1b-SC**. Ellipsoids are drawn at the 50% probability level, hydrogen atoms are shown as spheres of arbitrary radii.

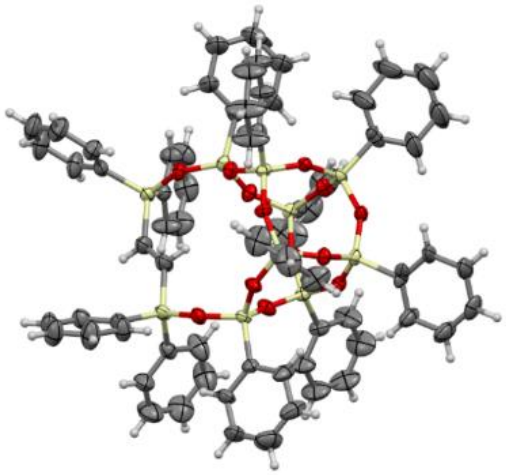

Figure S 58 A perspective view of the molecule **SQ-Td1c-SC**. Ellipsoids are drawn at the 50% probability level, hydrogen atoms are shown as spheres of arbitrary radii.

8. References

[1] CrysAlisPro 1.171.40.81a. 2020, p (Rigaku Oxford Diffraction)

[2] G.M. Sheldrick, *Acta Crystallogr. Sect. A Found. Crystallogr*. **2015**, *71*, 3–8.

[3] G. M. Sheldrick, *Acta Crystallogr. Sect. C Struct. Chem.* **2015**, *71*, 3–8.

[4] A. L. Spek, *Acta Crystallogr. Sect. C Struct. Chem.* **2015**, *71*, 9–18.

[5] K. Mituła, J. Duszczak, D. Brząkalski, B. Dudziec, M. Kubicki, B. Marciniec, *Chem. Commun.* **2017**, *53*, 10370–10373.

[6] V. Ervithayasuporn, X. Wang, Y. Kawakami, *Chem. Commun*. **2009**, 5130-5132.

[7] M. Walczak, R. Januszewski, M. Majchrzak, M. Kubicki, B. Dudziec, B. Marciniec, *New J. Chem.* **2017**, *41*, 3290–3296.

[8] K. Mituła, B. Dudziec, B. Marciniec, *J. Inorg. Organomet. Polym. Mater.*, **2018**, *28*, 500–507.